

Grüneisen Parameters: origin, identity and quantum refrigeration

Yi-Cong Yu,¹ Shizhong Zhang,^{2,*} and Xi-Wen Guan^{1,3,†}

¹*State Key Laboratory of Magnetic Resonance and Atomic and Molecular Physics,
Wuhan Institute of Physics and Mathematics, IAPMST,
Chinese Academy of Sciences, Wuhan 430071, China*

²*Department of Physics and Center of Theoretical and Computational Physics,
The University of Hong Kong, Hong Kong, China*

³*Department of Theoretical Physics, Research School of Physics and Engineering,
Australian National University, Canberra ACT 0200, Australia*

In solid state physics, the Grüneisen parameter (GP), originally introduced in the study of the effect of changing the volume of a crystal lattice on its vibrational frequency, has been widely used to investigate the characteristic energy scales of systems with respect to the changes of external potentials. On the other hand, the GP is little investigated in a strongly interacting quantum gas systems. Here we report on our general results on the origin of GP, new identity and caloric effects in quantum gases of ultracold atoms. We prove that the symmetry of the dilute quantum gas systems leads to a simple identity among three different types of GPs, quantifying caloric effect induced respectively by variations of volume, magnetic field and interaction. Using exact Bethe ansatz solutions, we present a rigorous study of these different GPs and the quantum refrigeration in one-dimensional Bose and Fermi gases. Based on the exact equations of states of these systems, we obtain analytic results for the singular behaviour of the GPs and the caloric effects at quantum criticality. We also predict the existence of the lowest temperature for cooling near a quantum phase transition. It turns out that the interaction ramp-up and -down in quantum gases provides a promising protocol of quantum refrigeration in addition to the usual adiabatic demagnetization cooling in solid state materials.

PACS numbers:

I. INTRODUCTION

The structure of energy spectrum of a quantum many-body system and its evolution under external perturbation characterises essentially its possible phases. As an example, the Grüneisen parameter (GP) [1, 2], which was introduced by Eduard Grüneisen in the beginning of 20th Century in the study of the effect of volume change of a crystal lattice on its vibrational frequencies, has been extensively studied for the exploration of caloric effect of solids and phase transitions associated with volume change. Similarly, the magnetic GP quantifies the magnetocaloric effect (MCE), establishing connection between refrigeration and variation of magnetic field.

So far, the GP has found diverse applications in geophysics [3, 4], chemical physics [5, 6], high pressure physics and plasma physics [7–9]. Recently, experiments also started to focus on GP in heavy-fermion systems [10–12], in which the physical properties at low temperatures are dominated by f -electrons and their antiferromagnetic exchange J with conduction electrons [13]. The heavy-fermion metals are extremely sensitive to a small change of pressure and this pressure sensitivity is reflected in highly enhanced values of the GP [14]. At low temperatures, divergence of the GP stronger than logarithmic upon cooling in the quantum regime is used for experimental identification of quantum critical points [10, 15–18].

The corresponding GPs in dilute quantum gases, how-

ever, are much less explored. In addition to the ability to change the volume of the system by modifying the external confining potential and the ability to change the equivalent magnetic field by changing population imbalance, it is also possible to change the interaction directly by using Feshbach resonance [19, 20]. This possibility suggests a new avenue for studying a novel interacting GP in addition to those defined by changes in volume and magnetic field [8, 11–16, 18, 21–26]. Furthermore, we establish an exact identity between these various GPs, making use of the scaling properties of the quantum gas system. The interaction driven caloric effect in quantum gases will also be discussed.

In this paper, we discuss the physical origin of GPs, establish a new identity and investigate the efficiency of quantum refrigeration by modifying the interaction strength in quantum gases. These GPs can be generally described by the ratio between the energy-pressure (or energy-magnetization and energy-contact) covariance and energy fluctuation, similar to the the Wilson ratio [27]. Using exact Bethe ansatz solutions, we show how interacting GP characterizes the quantum phase transitions for 1D quantum gases and demonstrate that the cooling effect is greatly enhanced near the quantum critical point. Our study shows promising route for studying interaction driven quantum heat engine and refrigeration in ultracold atoms.

II. THEORY: THE ORIGIN, GENERALIZATION AND NEW IDENTITY

1. The origin. There are many formulations of the GP to quantify the degree of anharmonicity on the structure of the energy spectrum in response to volume change. The original definition of the GP was introduced by E. Grüneisen for the Einstein model [1, 2],

$$\Gamma =: -\frac{V}{\omega_0} \frac{\partial \omega_0}{\partial V} = \frac{V}{C_V} \frac{\partial S}{\partial V}, \quad (1)$$

where the excitations in a solid is described by N phonons with the same frequency ω_0 . S is the entropy and V denotes the volume. In quantum statistical physics, the differential forms of the internal energy E and the pressure p can be represented by the fluctuations and covariances of thermodynamic quantities. If we regard the population a_i of the i -th energy level as a distribution function of a random variable and observable thermal quantities as the expectation value with respect to this distribution, then one can obtain the following differential relations, see supplementary material (SM) [28]

$$\begin{aligned} dE &= [-\text{Cov}(E, E)]d\beta + [-p + \beta \text{Cov}(p, E)]dV \\ dp &= [\text{Cov}(p, E)]d\beta + [E'' + \beta \text{Cov}(p, p)]dV, \end{aligned}$$

where Cov denotes the covariance and $E'' = \sum_i a_i \frac{\partial^2 \epsilon_i}{\partial V^2}$. $\beta = 1/(k_B T)$ and k_B is the Boltzman constant and T is the temperature. Then the GP is simply given by

$$\Gamma = -\frac{V \text{Cov}(p, E)}{\text{Cov}(E, E)} = \frac{V dp/d\beta|_V}{dE/d\beta|_V}. \quad (2)$$

Thus, in this case, Γ represents the relative importance of energy-pressure covariance and the energy fluctuation in the system. In contrast to the susceptibility (or compressibility) Wilson ratio proposed in [27, 29, 30], i.e., the ratio between the magnetization M (or particle number) fluctuation and the energy fluctuation, namely $R_W^\chi \propto \frac{\text{Cov}(M, M)}{\text{Cov}(E, E)}$ (or $R_W^\kappa \propto \frac{\text{Cov}(N, N)}{\text{Cov}(E, E)}$), the GP (2) provides additional insights into the spectral information with respect to the change of the volume of the system.

2. In grand canonical ensemble. In cold atom system, it is far more convenient to work in grand canonical ensemble and it is useful to derive the form of Γ in the grand canonical ensemble. Let μ be the chemical potential of the system and one finds

$$\Gamma = \frac{V \frac{dp}{dT}|_{V, N}}{\frac{dE}{dT}|_{V, N}} = \frac{1}{T} \frac{\frac{\partial^2 p}{\partial \mu^2} \frac{\partial p}{\partial T} - \frac{\partial^2 p}{\partial \mu \partial T} \frac{\partial p}{\partial \mu}}{\frac{\partial^2 p}{\partial \mu^2} \frac{\partial^2 p}{\partial T^2} - \left(\frac{\partial^2 p}{\partial \mu \partial T}\right)^2}, \quad (3)$$

In deriving the above equations, we applied the Maxwell's relations and used the homogeneous assumption that the grand thermal potential is a linear function of the volume neglecting the surface effect in the thermodynamic limit [31], i.e. $\Omega = -pV$ [63].

3. The effective and magnetic Grüneisen parameter. There is a widely used effective GP in experiment, defined as the ratio of thermal expansion parameter $\beta_T = \frac{1}{V} \frac{\partial V}{\partial T}|_{p, N}$ to the specific heat at a constant volume [11, 12, 14, 21, 26, 32]

$$\Gamma_{\text{eff}} = \frac{\beta_T}{c_V/V} = \Gamma \cdot \frac{\partial^2 p}{\partial \mu^2} \left(\frac{\partial p}{\partial \mu} \right)^{-2} = \Gamma \cdot \frac{\kappa}{n^2}, \quad (4)$$

here κ is the compressibility and n is the density. We denote it by "eff-Grüneisen parameter" since it is not equivalent to the original definition (3). In the above equation, the thermal expansion parameter in grand canonical ensemble can be given by

$$\beta_T = \left(\frac{\partial^2 p}{\partial \mu^2} \frac{\partial p}{\partial T} - \frac{\partial^2 p}{\partial \mu \partial T} \frac{\partial p}{\partial \mu} \right) \left(\frac{\partial p}{\partial \mu} \right)^{-2}. \quad (5)$$

Note that the usefulness of eff-GP is not well established in experiment; see the discussion on its divergent behaviour at quantum critical points [12, 14, 25]. However, it is clear that the eff-GP is not a dimensionless parameter and shows different scaling forms at the quantum critical points. To clearly show the dimensionless nature of the Grüneisen parameter, we define another dimensionless GP by [28]

$$\Gamma = \frac{V \frac{\partial S}{\partial V}|_{N, T}}{T \frac{\partial S}{\partial T}|_{N, V}} \quad (6)$$

which is equivalent to the definition (1), (2) and (3) and is intimately related to the expansionary caloric effect

$$\frac{\partial T}{\partial V} \Big|_{S, N, H} = \frac{T}{V} \Gamma. \quad (7)$$

In quantum statistics, the volume V of a system can be regarded as an external field that imposes a constrain on the particles. Therefore, it is natural to investigate other potentials that impose different constraints on the system. As a remarkable example, the well known magnetic GP discussed in experiments [14–16, 18] can be introduced analogously by replacing the volume V by the magnetic field H in the definition (6)

$$\Gamma_{\text{mag}} = -\frac{H \frac{\partial S}{\partial H}|_{N, T, V}}{T \frac{\partial S}{\partial T}|_{N, B, V}} \quad (8)$$

Here we added a minus sign following the former work [18, 33], and put the magnetic field H in the numerator in order to keep the GP dimensionless. It is straightforward to obtain the explicit form of the magnetic GP in grand canonical ensemble

$$\Gamma_{\text{mag}} = -\frac{H}{T} \frac{\frac{\partial^2 p}{\partial \mu^2} \frac{\partial^2 p}{\partial H \partial T} - \frac{\partial^2 p}{\partial \mu \partial H} \frac{\partial^2 p}{\partial \mu \partial T}}{\frac{\partial^2 p}{\partial \mu^2} \frac{\partial^2 p}{\partial T^2} - \left(\frac{\partial^2 p}{\partial \mu \partial T}\right)^2}. \quad (9)$$

The magnetic GP (8) plays an important roles in the experimental study of solid state materials [13, 18, 24, 32, 34].

One of the most important features of the magnetic materials is the magnetocaloric effect, related to the magnetocaloric refrigeration. In low temperature physics, this is known as adiabatic demagnetization cooling; see recent new developments [16, 17]. By the definition of the Γ_{mag} in eq. (8), we further get

$$\left. \frac{\partial T}{\partial H} \right|_{S,N,V} = \frac{T}{H} \Gamma_{\text{mag}}, \quad (10)$$

which establishes an important relation between magnetocaloric effect and the magnetic GP. Experimentally, it is easier to measure the magnetocaloric effect and from Eq. (10), obtain Γ_{mag} instead of using its original definition (8). One can obtain the magnetic entropy change $\partial S / \partial H|_{N,T,V}$ once we know the value of specific heat. The magnetic GP contains information free of any material-specific parameter [18].

4. The interacting Grüneisen parameter. In addition to the usual conjugate variables that one usually encounters in thermodynamics, in ultracold atomic gases, it is also possible to define another set of conjugate variable related to the interaction between atoms. In the case of s -wave interacting system, the low-energy scattering properties are determined entirely by the s -wave scattering length a_s . In one-dimensional system, the 1D coupling constant c is related to the scattering length ($c \propto a_s^{-1}$). In reality, it is possible to change the scattering length a_s by using Feshbach resonance and one can define analogously another GP related to interaction

$$\Gamma_{\text{int}} = -\frac{c \frac{\partial S}{\partial c} |_{N,H,T,V}}{T \frac{\partial S}{\partial T} |_{N,H,c,V}} = -\frac{\frac{\partial^2 p}{\partial \mu^2} \frac{\partial^2 p}{\partial c \partial T} - \frac{\partial^2 p}{\partial \mu \partial c} \frac{\partial^2 p}{\partial \mu \partial T}}{\frac{\partial^2 p}{\partial \mu^2} \frac{\partial^2 p}{\partial T^2} - \left(\frac{\partial^2 p}{\partial \mu \partial T} \right)^2} \frac{c}{T}. \quad (11)$$

The physical significance of Γ_{int} is that it describes the caloric effect due to modification of interaction strength. In particular, in an isentropic process, one can relate the change of temperature to interaction strength given by

$$\left. \frac{\partial T}{\partial c} \right|_{S,N,V,H} = \frac{T}{c} \Gamma_{\text{int}}. \quad (12)$$

This is an interaction analog of the magnetocaloric effect. We observe that from eq. (12) that a heat engine and quantum refrigeration can be constructed by tuning the interaction strength in quantum gases. Therefore the interaction gradients are capable of cooling the system of interacting fermions like the magnetization gradient cooling [35, 36]. We shall further discuss interaction driven quantum refrigeration in next section.

5. Universal identity. So far we have presented three different GPs, i.e., Γ , Γ_{mag} and Γ_{int} , which quantify the degrees of anharmonicity of spectral structures in

regard of the variations of volume, magnetic field and interaction strength, respectively. Using the general thermal potential [37], one can find a new identity for the three GPs for dilute system described by s -wave scattering length a_s [19]. For these systems, one has the following scaling transformations: $L \rightarrow e^\lambda L, c \rightarrow e^{\chi\lambda} c, H \rightarrow e^{-2\lambda} H$, where e^λ is the scaling amplitude and the χ is the exponent of the dependency of the coupling strength and the scattering length by $c \propto a_s^\chi$, then we find that the spectrum of such quantum many-body systems will be changed by $\epsilon_n \rightarrow e^{-2\lambda} \epsilon_n$, here ϵ_n denotes the n -th energy level. Meanwhile, if the temperature transforms as $T \rightarrow e^{-2\lambda} T$, the population $a_n = e^{-\frac{\epsilon_n}{T}} / \sum_i e^{-\frac{\epsilon_i}{T}}$ is invariant under such scaling transformations, and so does the entropy $S = -\sum a_i \ln a_i$, i.e.

$$0 = dS = \left. \frac{\partial S}{\partial V} \right|_{T,H,c} dV + \left. \frac{\partial S}{\partial T} \right|_{V,H,c} dT + \left. \frac{\partial S}{\partial H} \right|_{V,T,c} dH + \left. \frac{\partial S}{\partial c} \right|_{V,T,H} dc.$$

Substituting the scaling transformations into the above equation and noticing $V = L^d$ with d being the dimension of the system, we obtain an important identity

$$dV \left. \frac{\partial S}{\partial V} \right|_{T,H,c} = 2T \left. \frac{\partial S}{\partial T} \right|_{V,H,c} + 2H \left. \frac{\partial S}{\partial H} \right|_{V,T,c} - \chi c \left. \frac{\partial S}{\partial c} \right|_{V,T,H}$$

that relates the entropy changes to the variations of the interaction, magnetic field and the volume of the system. Using the definitions of GPs given in eqs. (1), (8) and (11), we obtain a simple identity

$$d\Gamma + 2\Gamma_{\text{mag}} - \chi\Gamma_{\text{int}} = 2. \quad (13)$$

In one dimension systems we have $d = 1$ and $\chi = -1$ [38], the identity above is reduced to $\Gamma + 2\Gamma_{\text{mag}} + \Gamma_{\text{int}} = 2$. Although we obtained this identity through the scaling invariance of the entropy, it is universal and valid for quantum gases in 1D and higher dimensions. We can prove this identity (13) in a more conventional way of quantum statistical physics, see [28]. This identity eq. (13) has many interesting applications. The term $2/d$ in eq. (13) gives the nature of the scaling invariant spectrum of ideal gases, also see the discussion on the Grüneisen parameter, where it is exactly $\frac{2}{3}$ for 3D free gas [39], obviously corresponding to a special case of eq. (13) with $d = 3$ and $\Gamma_{\text{mag}} = \Gamma_{\text{int}} = 0$. A further study of the identity (13) will be published elsewhere [64].

III. APPLICATIONS: QUANTUM CRITICALITY AND QUANTUM REFRIGERATION

1. Magnetic and interaction driven refrigeration. Through the study presented in last section, we

have shown that it is possible to reduce the temperature of a magnetic system by changing the external magnetic field in an isentropic process. Based on this magnetocaloric effect, it is possible to cool the systems into extremely low temperatures via either spin flipping or magnetic field gradient (spin transport) [35, 36]. Other refrigerators are also discussed [40, 41].

In cold atomic gas systems, however, inter-conversion between different spin (hyperfine) states is very slow and the usual magnetic cooling is inefficient. In addition, the corresponding external magnetic field is given by the difference between chemical potentials of two spin states, which is not possible to alter in experiments. On the other hand, it is possible to construct a corresponding cooling process much like the magneto caloric effect based on the modification of interaction parameter based on the analogy between Eqs. (10) and (12). However, before we discuss the interaction induced cooling, let us first review the standard magnetic refrigeration.

In the magnetic refrigeration cycle, depicted in Fig. 1, there are four processes. $A \rightarrow B$: initially randomly oriented magnetic moments are aligned by a magnetic field, resulting in the heating of the magnetic material; $B \rightarrow C$: heat is removed from the medium to the hot bath by coupling the working medium and the hot bath; $C \rightarrow D$: by removing away the magnetic field adiabatically, the magnetic moments are randomized, that leads to cool the material below the cold ambient temperature, and finally $D \rightarrow A$: heat is extracted from the cold ambient to the working medium by coupling the working medium and the target. This technique is also referred to the adiabatic demagnetization refrigerator (ADR) as being shown in the key step $C \rightarrow D$, where the working system is demagnetized adiabatically. In the process $B \rightarrow C$ the total heat absorbed by the ambient from the working system is the area of the curved trapezoid $BCEF$, i.e. $\Delta Q_1 = S_{BCEF}$, and similarly in the process $D \rightarrow A$ the total heat that is absorbed from the target system is $\Delta Q_2 = S_{ADEF}$. The cooling efficiency of the refrigerator is $\eta = \Delta Q_2 / \Delta Q_1$, which imply that the limitation of the efficiency is $\eta_{\max} = T_{\text{tar}} / T_{\text{sour}}$ when $T_B \rightarrow T_c$ and $T_A \rightarrow T_D$. But the maximum of the efficiency means the minimal of the power. For a realistic application, one has to weight the efficiency and the power. In low temperature physics, the reachable low temperature limit is the most important issue for engineering refrigeration. We shall further discuss the possible lowest temperature for a cooling by near a quantum phase transition. Below, we construct the analogous magnetic refrigeration cycle based on changing interaction parameters.

To make concrete the above statement, we demonstrate quantum refrigeration based on the Bethe ansatz solution of the Lieb-Liniger model, which describes the 1D Bose gas with a contact interaction. The Hamiltonian of the Lieb-Liniger model in a 1D box with length

L is given by [42]

$$\hat{H} = -\frac{\hbar^2}{2m} \sum_{i=1}^N \frac{\partial^2}{\partial x_i^2} + 2c \sum_{1 \leq i < j \leq N} \delta(x_i - x_j). \quad (14)$$

where m is the mass of the particles, c is the coupling strength which is determined by the 1D scattering length $c = -2\hbar^2 / ma_{1D}$. The scattering length is given by $a_{1D} = (-a_{\perp}^2 / 2a_s)[1 - C(a_s/a_{\perp})]$ [38, 43, 44].

Before analysing the refrigerator cycle, we first briefly study the thermodynamic scaling invariance of this model. In order to prove the scaling invariant nature in the entropy, here we extend our discussion presented in the last section to the exactly solved model. The Hamiltonian (14) can be solved by Bethe ansatz [42, 45], we list some related key results in [28]. Suppose that we have obtained the solution of the thermodynamic Bethe ansatz equation (S30) of dressed energy $\epsilon(k)$ under the input parameters μ , T and c , it is obvious that the dressed energy $\epsilon'(k') = e^{-2\lambda}\epsilon(e^{\lambda}k')$ is the corresponding scaling form for input parameters under such rescaling $T' = e^{-2\lambda}T$, $\mu' = e^{-2\lambda}\mu$ and $c' = e^{-\lambda}c$. Strictly speaking, the dressed energy is a homogeneous function with $\epsilon(e^{\lambda}k, e^{-2\lambda}\mu, e^{-2\lambda}T, e^{-\lambda}c) = e^{-2\lambda}\epsilon(k, \mu, T, c)$ for $\forall \lambda \in R$. By definition [28], the pressure can be obtained in a straightforward way, i.e. we may obtain an homogeneous form of the pressure $p(e^{-2\lambda}\mu, e^{-2\lambda}T, e^{-\lambda}c) = e^{-3\lambda}p(\mu, T, c)$. By differentiation, the density is given by $n(e^{-2\lambda}\mu, e^{-2\lambda}T, e^{-\lambda}c) = e^{-\lambda}n(\mu, T, c)$. Furthermore, the the entropy density $s = S/L$ is given by

$$s(e^{-2\lambda}\mu, e^{-2\lambda}T, e^{-\lambda}c) = e^{-\lambda}s(\mu, T, c). \quad (15)$$

For the system with the fixed particle number, we need $L \rightarrow L' = e^{\lambda}L$ to ensure $N' = N$ under scaling transformation $\mu' = e^{-2\lambda}\mu$, $T' = e^{-2\lambda}T$, $c' = e^{-\lambda}c$, then according to (15) we arrive at the conclusion that under this scaling transformation the entropy is unchanged $S' = S$ which is the key conclusion we have claimed to obtain the identity of Grüneisen parameters (13) in the last section.

Similar discussions can be given on Gaudin-Yang model (see next section) and other integrable models. However, we emphasize that the identity (13) does not depend on any particular model and has its origin in the scaling properties of the spectrum. Historically, the study of the Grüneisen parameter started, in fact, from the discussion on homogeneity of thermodynamic quantities as functions of the oscillation frequency ω_0 in the simple Einstein model [1, 2] (for details, see supporting material [28]).

Now let us return to our discuss on refrigerator cycle driven by the interaction strength c in the Lieb-Liniger model (14). As a direct analogy to Fig. 1, the interaction driven refrigerator cycle is showed in the $T-S$ and $T-c$ plane in Fig. 2 via rigorous calculation by thermodynamic Bethe ansatz equations, see [28]. The implementation

(a) Schematics

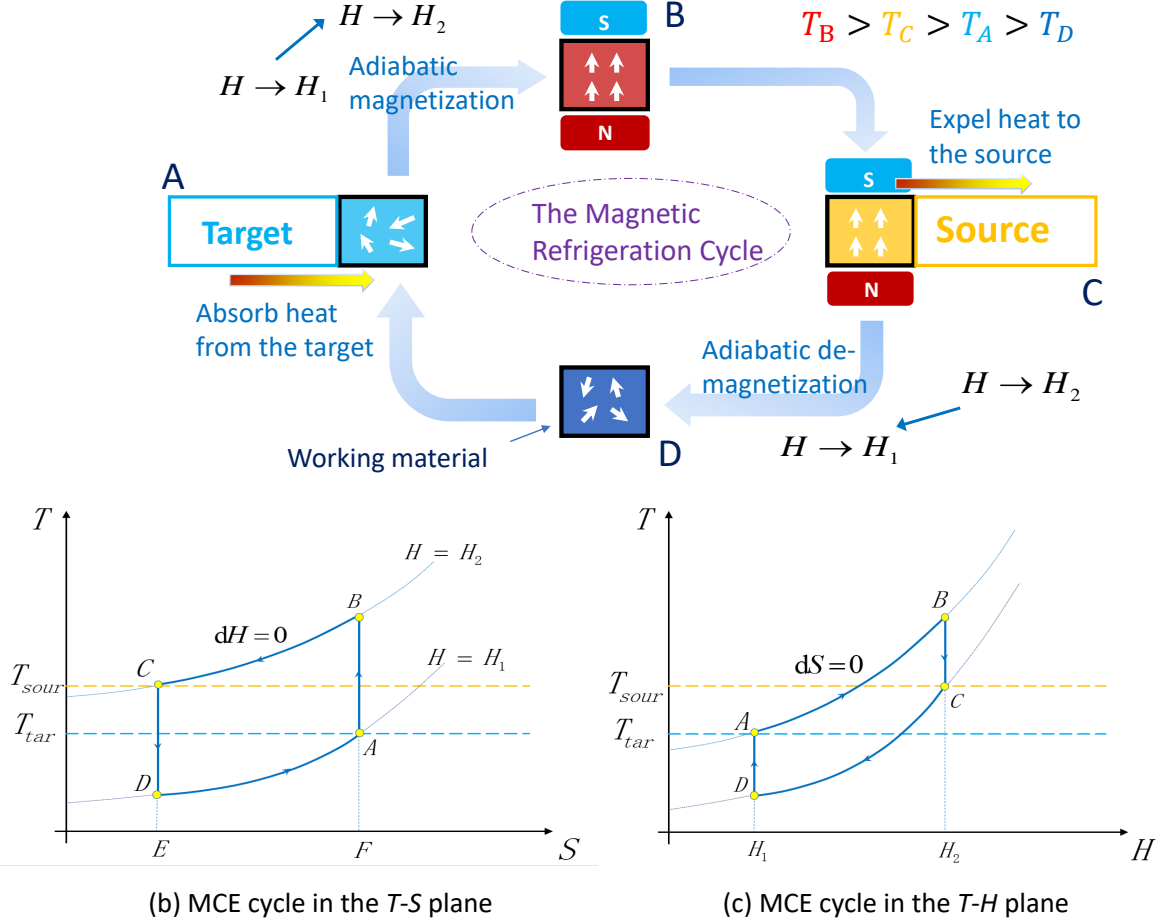


FIG. 1: Schematic representation for the magnetic refrigeration cycle: (a) The working circle between the target and the heat source absorbs heat from the target at a lower temperature T_{tar} and transfers heat to the source at a higher temperature T_{sour} . Different colors label different temperatures. At the point B and C, a strong magnetic field is applied and the material is polarized sufficiently. Whereas at the point A and D, the material is demagnetized. (b) The magnetic refrigeration cycle in the $T-S$ plane and (c) in the $T-H$ plane. $B \rightarrow C$ and $D \rightarrow A$ are isomagnetic processes with $dH = 0$, and $A \rightarrow B$ and $C \rightarrow D$ are isentropic. The whole processes $A \rightarrow B \rightarrow C \rightarrow D \rightarrow A$ were discussed in detail the main text. In $D \rightarrow A$, the heat is absorbed by the working material from the target. In the process $B \rightarrow C$, the heat is expelled from the working material to the heat source.

of such as cycle by dunning the interaction in the 1D interacting Bose gas much likes the interaction driven heat engine proposed in [46].

The right panel of Fig. 2 shows the four strokes in a cooling cycle with the interacting bosons. $A \rightarrow B$: The working medium is initially in the thermal state A determined by the interaction strength $c_A = 1$ and temperature $T_{tar} = 1$. The isentropic ramp-up of interaction takes place and the interaction strength is finally enhanced to the value c_B . After a quasi-adiabatic unitary evolution, the system reaches to a state with temperature T_B . $B \rightarrow C$: Keeping c_B constant, the working medium is coupled to the hot ambient at temperature T_{sour} and reaches the equilibrium state (c_B, T_{sour}) . The

heat ΔQ_1 is removed from the working medium into the hot ambient. $C \rightarrow D$: The working medium is decoupled from the hot ambient. By performing a work, interaction ramp-down isentropic process takes place. The interaction strength decreases from c_B to $c_D = c_A$, the working medium reaches the temperature T_D . $D \rightarrow A$: The working medium is coupled to the target cold reservoir keeping the interaction strength constant until it reaches the thermal state (c_A, T_{tar}) . The heat ΔQ_2 is extracted from the target reservoir. The cooling efficiency is $\eta = \Delta Q_2 / \Delta Q_1$.

We would like to stress that in a realistic cycle, $A \rightarrow B$ and $C \rightarrow D$ are likely not to be rigorously adiabatic. However, the temperatures at the non-thermal state B and D can be still well defined if the spectra of the

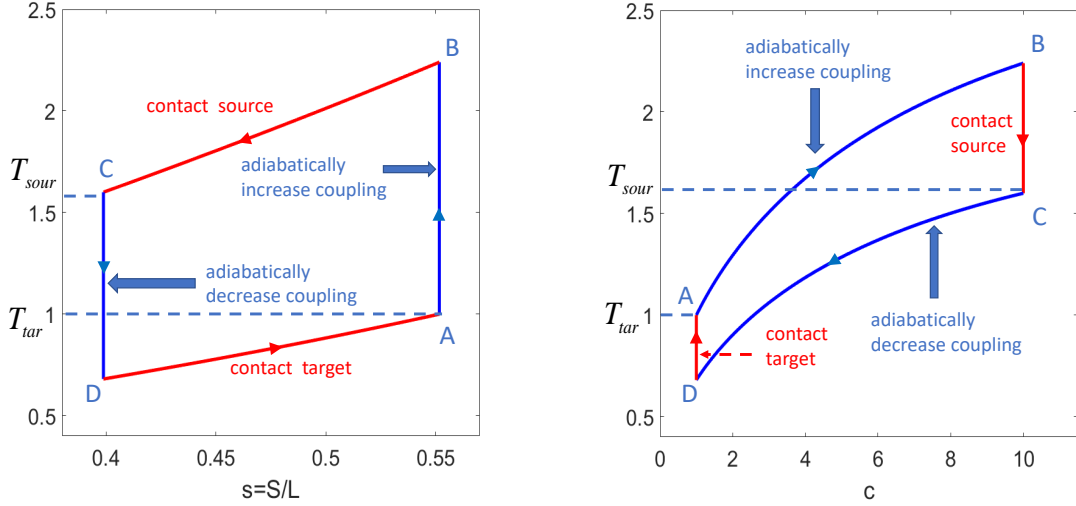


FIG. 2: Schematic demonstration of the interaction driven refrigeration in the $T-s$ and $T-c$ planes. The cycle with four processes is an analog to the magnetic refrigeration which we discussed in the Fig. 1. Here the processes: $A \rightarrow B$: interaction ramp-up isentrope; $B \rightarrow C$: an isochore by contacting a hot source (release heat to the hot source); $C \rightarrow D$: interaction ramp-down isentrope; $D \rightarrow A$: a isochore by contacting a cold source (absorb heat from the target source). The cycle is plotted by numerically solving the thermodynamic Bethe ansatz equations (TBAE) of the Lieb-Linger model, see [28]. The cycle begins at point A with $n = 0.1, c = 1.0, T = 1.0$, (here all the quantities are in the nature units $\hbar = 2m = k_B = 1$.) then the coupling strength is tuned to strong interacting region $c = 10.0$, after contacting with the heat source the coupling strength is tuned back to $c = 1.0$, finally the working material contacts sufficiently to the target, and the cycle is finished.

working system are scaling invariant, see discussion in Ref.[46]. The exact solution of the working system allows us to determine working efficiency in this particular case. We would like to mention that the modulation of the coupling strength in an interaction-driven cooling cycle can be associated with the coupling to external degrees of freedom, also see a recent study of the quantized refrigerator [47]. In next section, we shall discuss the reachable lowest temperature for an engineering refrigeration with the 1D interacting fermions.

2. The Grüneisen parameter at quantum criticality. As discussed in the last section, the Grüneisen parameters play the central role in this cooling process based on the equations (10) or (12). Since the Grüneisen parameters are second order derivatives with respect to free energy, it is expected that the Grüneisen parameters will show divergent and scaling behaviors at the QCPs [13, 14, 17, 18, 24, 32, 34], leading to much enhanced effects for quantum refrigeration.

In order to illustrate this idea and to analyse the scaling behaviors of the GPs, we take the Yang-Gaudin model [48, 49] as an example to carry out rigorous calculations. This model is one of the most important exactly solvable quantum many-body systems. It was solved long ago by Yang [48] and Gaudin [49] using the

Bethe ansatz. Theoretical predictions for the existence of a Fulde-Ferrell-Larkin-Ovchinnikov (FFLO) pairing state in the 1D interacting Fermi gas have emerged by using the exact solution [50–52]. The key features of this $T = 0$ phase diagram were experimentally confirmed using finite temperature density profiles of trapped fermionic ^6Li atoms [53]. The Hamiltonian of the Yang-Gaudin model

$$\begin{aligned} \hat{H} = & \sum_{\sigma=\downarrow,\uparrow} \int \phi_{\sigma}^{\dagger}(x) \left(-\frac{\hbar^2}{2m} \frac{d^2}{dx^2} + \mu_{\sigma} \right) \phi_{\sigma}(x) dx \\ & + g_{1D} \int \phi_{\downarrow}^{\dagger}(x) \phi_{\uparrow}^{\dagger}(x) \phi_{\uparrow}(x) \phi_{\downarrow}(x) dx \\ & - \frac{1}{2} \hbar \int \left(\phi_{\uparrow}^{\dagger}(x) \phi_{\uparrow}(x) - \phi_{\downarrow}^{\dagger}(x) \phi_{\downarrow}(x) \right) dx \quad (16) \end{aligned}$$

describes a 1D δ -function interacting two-component Fermi gas of N fermions with mass m and an external magnetic field H constrained by periodic boundary conditions to a line of length L . Where $g_{1D} = -2\hbar^2/(ma_{1D})$ is determined by an effective scattering length a_{1D} via Feshbach resonances or confinement-induced resonances [38, 43, 44]. $g_{1D} > 0$ (< 0) represents repulsive (attractive) interaction. Usually $c = mg_{1D}/\hbar^2 = -2/a_{1D}$ denotes the effective interaction strength.

Here we show that the different GPs (3), (9) and (11) not only signal quantum phase transitions but also quan-

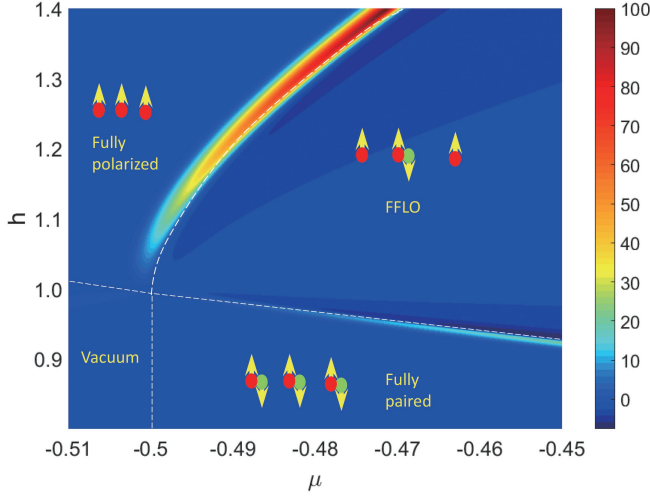


FIG. 3: Contour plot of the negative GP (3), i.e. $-\Gamma$, mapping out the full phase diagram of the Yang-Gaudin model with an attractive interaction in $h-\mu$ plane. It consists of three novel phases, fully paired state, Fully polarized state and a FFLO like state. Here the dimensionless temperature $t = 0.001$. The GP has a sudden enhancement near the phase boundaries, giving a universal divergent scaling $\Gamma \sim t^{-1/2}$, see the main text.

tify various fluctuations in quantum systems. Using the exact TBA equations, a full critical phase diagram of the Yang-Gaudin model at $t = 0.0001\epsilon_b$ is determined by the GP expression (3), see supplementary material [28]. In this contour plot the rescaled units were used, i.e. $\tilde{t} = t/(c^2/2)$, $\tilde{\mu} = \mu/(c^2/2)$ and $\tilde{h} = h/(c^2/2)$. We observe that the GP (3) characterizes the universal divergent scaling near the phases boundaries. It shows that the energy-pressure covariance has a stronger fluctuations than the energy fluctuation. This nature can be used to identify different quantum phases, i.e. novel Luttinger liquids of fully-paired state, FFLO-like pairing state and fully polarized state are determined at low temperatures, see Fig. 3. We show that the phase boundaries between the fully polarized phase and FFLO-like pairing phase and between the fully paired phase and FFLO-like pairing phase in Fig. 3 can be cast into a universal scaling (for a constant h)

$$\Gamma = \lambda t^{-1/2} \mathcal{G}\left(\frac{2(\mu - \mu_c)}{t}\right) \quad (17)$$

with the factor $\lambda = \sqrt{\pi}n$ and $\lambda = \sqrt{2\pi}n$, respectively. In the above equation, n is the density, $\mathcal{G}(x)$ is the scaling function and μ is an effective chemical potential [20]. More detailed study on the quantum scalings of the GPs (17) will be published elsewhere. In addition, the magnetic and interacting GPs (9) and (11) also give the full phase diagram at low temperatures.

The divergence of the GPs at $T \rightarrow 0$ near QCPs can

be clearly understood by investigating the entropy of the system. At low temperatures, the state of the system away from the critical points usually behaves like Fermi liquid (or Tomonaga-Luttinger liquid region in 1D), see Fig. 3. The entropy $S \propto T$. In contrast, the entropy at the quantum criticality behaves as [54, 55]

$$\frac{S}{V} \propto T^{(d/z)+1-(1/\nu z)} \mathcal{K}\left(\frac{\mu - \mu_c}{T^{1/\nu z}}\right). \quad (18)$$

For 1D system, $z = 2$ is the dynamic critical exponent and $\nu = 1/2$ is the critical index for correlation length, whereas the μ presents an effective chemical potential, and the μ_c is the quantum critical point. $\mathcal{K}(x)$ is some analytical scaling function. Note that the entropy is exactly zero at zero temperature, so there is no background term in eq. (18) [20, 29, 30, 37, 56, 57]. For the Gaudin-Yang model, the entropy $S \propto \sqrt{T} \gg T$ near the QCPs, which implies the local maximum of the entropy at QCPs. If we plot the entropy in the $T-H$ plane, see Fig. 4, the isentropic lines will be bent down significantly at QCPs. According to equation (10), the GPs are proportional to the slope of the isentropic line which leads to the divergence of the GP when $T \rightarrow 0$.

The local maximum of the entropy at low temperature reveals the essence of the QCPs when the low lying excitation becomes degenerate with the ground state [58]. In general, the divergence of the GPs is also present in generic models when quantum phase transition occurs. This nature has been extensively studied both in theory and experiments [10–16, 18, 21, 23, 32–34, 59, 60].

3. Quantum refrigeration near a phase transition. For refrigeration, it is important to ask what the lowest temperature one can achieve. In Supplementary material [28], we answer the above question for the free Fermi gas. This question seems trivial in the common refrigeration [23]. However, if the system approaches its quantum critical point, things can be significantly different. The divergent behaviour of the GPs near QCPs can lead to significant cooling of the system. In fact, the feature of local maximum of the entropy leads to a local temperature minimum in an isentropic process, see Fig. 4. Consequently, one can take this advantage of the quantum phase transition to enhance the MCE (or interaction driven MCE). Using exact solution of the 1D attractive Fermi gas, we further demonstrate a magnetic (or interaction driven) refrigeration in the interacting Fermi gas [48, 49].

Using the condition (see the equation (10))

$$\Gamma_{\text{mag}} = 0, \quad (19)$$

we may answer the above question. For the Yang-Gaudin model [28], we expect an enhancement of the cooling efficiency when the working system is approaching to a quantum critical point in the phase diagram Fig. 3. Here we focus on the low temperature region, i.e. $T \ll T_d$, here

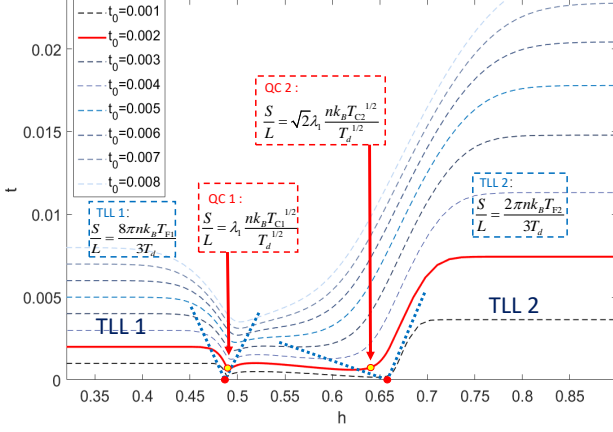


FIG. 4: The contour plot of the entropy in $t - h$ plane for the attractive Yang-Gaudin model at low temperatures. Here the magnetic field $h = H/\epsilon_b$ and the temperature $t = T/\epsilon_b$ are rescaled by the binding energy with $2m = \hbar = k_B = 1$. We carried out our calculation through the TBA equations [28] with a fixed density $n = 0.1$. h_{c1} and h_{c2} are the critical points for the phase transitions from fully paired TLL to the FFLO like phase and from the FFLO like phase to the fully polarized phase at $t = 0$, respectively. The dash lines in different colors present the contour values of entropies at different temperatures. The bending down of the contour lines indicates an entropy accumulation with a minimum temperature (yellow dot). For $h < h_{c1}$ the system is in the TLL of bound pairs obeying the state equation (22), whereas for $h > h_{c2}$ the system is in a fully polarized TLL obeying the equation (22). These analytical results of the state equations directly give the minima of the temperature during the adiabatic demagnetization processes, see (23).

$k_B T_d = (\frac{\hbar^2 n^2}{2m})$ is the degenerate temperature. Fig. 4 shows that the condition $\Gamma_{\text{mag}} = 0$ gives solutions for each quantum phase transition. Like the free Fermi gas given in [28], the condition $\Gamma_{\text{mag}} = 0$ leads to two independent equations for the Yang-Gaudin model at the two quantum critical points, namely,

$$-\frac{1}{2}\text{Li}_{\frac{1}{2}}(-e^{\tilde{A}^{(r)}/t}) + \frac{\tilde{A}^{(r)}}{t}\text{Li}_{-\frac{1}{2}}(-e^{\tilde{A}^{(r)}/t}) = 0, \quad (20)$$

where $r = 1$ and $r = 2$ stand for the unpaired fermions and bound pairs, respectively. This means that at the phase transition H_{c1} the density of state of unpaired fermions is suddenly changed, whereas at the critical point H_{c2} the density of state of the paired fermions is suddenly changed. While the effective chemical potentials of unpaired fermion and pairs, here $\tilde{A}^{(1)} = (\mu + H/2)/\epsilon_b$, $\tilde{A}^{(2)} = (2\mu + c^2/2)/\epsilon_b$ were rescaled by the bonding energy $\epsilon_b = c^2/2$. Here μ is the chemical potential, $t = T/\epsilon_b$ is the rescaled temperature.

Equation (20) is very similar to the equation $\mathcal{Y}(x) = x - \frac{\text{Li}_{1/2}(-e^x)}{2\text{Li}_{-1/2}(-e^x)} = 0$ found in the free Fermi gas [28]. We thus have the same solution $\tilde{A}^{(r)}/t = x_0 \approx 1.3117$. Sub-

stituting this solution into TBA results given in [28], we get entropies at the phase transitions point from a fully-paired phase to the FFLO-like state and from the FFLO-like state to the fully paired Fermi gas, respectively

$$\begin{aligned} \frac{S}{L} &= \lambda_1 \cdot \frac{\sqrt{m}}{\hbar\sqrt{2\pi}} k_B^{3/2} T_{c1}^{1/2}, \quad \text{for } H \rightarrow H_{m1} \\ \frac{S}{L} &= \lambda_1 \cdot \frac{\sqrt{m}}{\hbar\sqrt{\pi}} k_B^{3/2} T_{c2}^{1/2}, \quad \text{for } H \rightarrow H_{m2}, \end{aligned} \quad (21)$$

where $\lambda_1 = x_0 \text{Li}_{1/2}(-e^{x_0}) - \frac{3}{2}\text{Li}_{3/2}(-e^{x_0}) \approx 1.3467$. H_{m1} and H_{m2} are two critical fields corresponding to the two temperature minima in the isentropic contour lines. Using TBA equation, we have the entropy in the liquid phases of pairs and fully-polarized fermions

$$\begin{aligned} \frac{S}{L} &= \frac{4m}{3\hbar^2} k_B^2 T_{L1} n^{-1}, \quad \text{for } H < H_{m1}, \\ \frac{S}{L} &= \frac{m}{3\hbar^2} k_B^2 T_{L2} n^{-1}, \quad \text{for } H > H_{m2}. \end{aligned} \quad (22)$$

Here T_{L1} and T_{L2} are the temperatures in the Luttinger liquid regions, see the phases $TLL1$ and $TLL2$ in Fig. 4. For the first equation in (22), we applied the strong coupling condition $\gamma = c/n \gg 1$. From these equations (21) and (22), we find two temperature minima of the refrigeration around the two phase transitions

$$\begin{aligned} \frac{T_{c1}}{T_d} &= 8\lambda_2^2 \cdot \left(\frac{T_{L1}}{T_d}\right)^2, \\ \frac{T_{c2}}{T_d} &= \frac{\lambda_2^2}{2} \cdot \left(\frac{T_{L2}}{T_d}\right)^2 \end{aligned} \quad (23)$$

with $\lambda_2 = \frac{2\pi}{3\lambda_1} \approx 1.5552$. We further observe that the leading contribution to the entropy at the critical point H_{m1} involves the excitations of the excess fermions [29]. Whereas at the critical point H_{m2} , the leading contribution to the entropy comes from the excitations of the bound pairs. In the isentropic process, the system thus can retain more entropy per unit temperature near the finite temperature critical point H_{m2} . This result reveals an enhancement of the cooling efficiency. In cold atom experiment, the temperature is usually much lower than the degenerate temperature [61], i.e. $T_{L1}/T_d \ll 1$ and $T_{L2}/T_d \ll 1$. From equation (23), we thus have $T_{c1} \ll T_{L1}$ and $T_{c2} \ll T_{L2}$. Moreover, the ideal limit of the temperature $T_{c1,2}$ for the refrigeration is twice in order of magnitude compared to the temperature of the heat source $T_{L1,2}$.

IV. SUMMARY

We have conducted a comprehensive investigation of the GP for ultracold quantum gases, including its origin, new identity, caloric effects and quantum refrigeration. We have proposed the interaction related GP

which reveals characteristic energy scales of quantum system induced by the variation of the interaction. Together with the other two GPs related to the variations of volume and magnetic field, we have established a new identity between them which characterises the universal scalings of fluctuations and caloric effect in quantum gases. Based on the entropy accumulation at the quantum critical point, two promising protocols of quantum refrigeration driven either by interaction or by magnetic field have been studied. Using Bethe Ansatz, we studied the expansionary, the magnetic and the interacting GPs, quantum refrigeration, magnetocaloric effect and quantum critical phenomenon of the Lieb-Liniger model and Yang-Gaudin model. Our method opens to further study the GPs and quantum refrigeration for quantum gases of ultracold atoms with different spin symmetries in 1D and higher dimensions.

Acknowledgement

The author thanks Y.X. Liu, L. Peng, Y.Z. Jiang, Y.Y. Chen, F. He, H. Pu and R. Hulet for helpful discussions. This work is supported by the National Key R&D Program of China No. 2017YFA0304500, the key NSFC grant No.11534014 and No. 11804377. YCY thank the University of Hong Kong for a kind hospitality. XWG acknowledge Rice University for a support of his visit.

* shizhong@hku.hk

† e-mail:xwe105@wipm.ac.cn

- [1] E. Grüneisen. Über die Thermische Ausdehnung und die Spezifische Wärme der Metalle. *Annalen der Physik*, 331(6):211–216, 1908.
- [2] E. Grüneisen. Theorie des Festen Zustandes Einatomiger Elemente. *Annalen der Physik*, 344(12):257–306, 1912.
- [3] F. D. Stacey. Theory of thermal and elastic properties of the lower mantle and core. *Physics of the Earth and Planetary Interiors*, 89(3):219–245, 1995.
- [4] J. Shanker, K. Sunil, and B. S. Sharma. The Grüneisen parameter and its higher order derivatives for the earth lower mantle and core. *Physics of the Earth and Planetary Interiors*, 262:41–47, 2017.
- [5] P. Mausbach, A. Koster, G. Rutkai, M. Thol, and J. Vrabec. Comparative study of the Grüneisen parameter for 28 pure fluids. *Journal of Chemical Physics*, 144(24), 2016.
- [6] G. Liu, J. Zhou, and H. Wang. Anisotropic thermal expansion of SnSe from first-principles calculations based on Grüneisen’s theory. *Physical Chemistry Chemical Physics*, 19(23):15187–15193, 2017.
- [7] L. Wang, M. T. Dove, K. Trachenko, Y. D. Fomin, and V. V. Brazhkin. Supercritical Grüneisen parameter and its universality at the Frenkel line. *Physical Review E*, 96(1), 2017.
- [8] S. Kumar, S. K. Sharma, and O. P. Pandey. Brief report: volume dependence of Grüneisen parameter for solids under extreme compression. *Pramana-Journal of Physics*, 87(2), 2016.
- [9] S. A. Khrapak. Grüneisen parameter for strongly coupled Yukawa systems. *Physics of Plasmas*, 24(4), 2017.
- [10] R. Kuchler, N. Oeschler, P. Gegenwart, T. Cichorek, K. Neumaier, O. Tegus, C. Geibel, J. A. Mydosh, F. Steglich, L. Zhu, and Q. Si. Divergence of the Grüneisen ratio at quantum critical points in heavy fermion metals. *Physical Review Letters*, 91(6), 2003.
- [11] R. Kuchler, P. Gegenwart, J. Custers, O. Stockert, N. Caroca-Canales, C. Geibel, J. G. Sereni, and F. Steglich. Quantum criticality in the cubic heavy-Fermion system $\text{CeIn}_{3-x}\text{Sn}_x$. *Physical Review Letters*, 96(25):256403, 2006.
- [12] R. Kuchler, P. Gegenwart, C. Geibel, and F. Steglich. Systematic study of the Grüneisen ratio near quantum critical points. *Science and Technology of Advanced Materials*, 8(5):428–433, 2007.
- [13] P. Gegenwart. Grüneisen parameter studies on heavy fermion quantum criticality. *Reports on Progress in Physics*, 79(11), 2016.
- [14] A. Steppke, R. Kuchler, S. Lausberg, E. Lengyel, L. Steinke, R. Borth, T. Lühmann, C. Krellner, M. Nicklas, C. Geibel, F. Steglich, and M. Brando. Ferromagnetic quantum critical point in the heavy-Fermion metal $\text{YbNi}_4(\text{p}_{1-x}\text{a}_{1-x})$. *Science*, 339(6122):933–936, 2013.
- [15] Y. Tokiwa, T. Radu, C. Geibel, F. Steglich, and P. Gegenwart. Divergence of the magnetic Grüneisen ratio at the field-induced quantum critical point in YbRh_2Si_2 . *Physical Review Letters*, 102(6):066401, 2009.
- [16] B. Wolf, Y. Tsui, D. Jaiswal-Nagar, U. Tutsch, A. Honecker, K. Remoň-Langer, G. Hofmann, A. Prokofiev, W. Assmus, G. Donath, and M. Lang. Magnetocaloric effect and magnetic cooling near a field-induced quantum-critical point. *Proceedings of the National Academy of Sciences*, 108(17):6862, 2011.
- [17] B. Wolf, A. Honecker, W. Hofstetter, U. Tutsch, and M. Lang. Cooling through quantum criticality and many-body effects in condensed matter and cold gases. *International Journal of Modern Physics B*, 28(26), 2014.
- [18] H. Ryll, K. Kiefer, C. Ruegg, S. Ward, K. W. Kramer, D. Biner, P. Bouillot, E. Coira, T. Giamarchi, and C. Kollath. Magnetic entropy landscape and Grüneisen parameter of a quantum spin ladder. *Physical Review B*, 89(14), 2014.
- [19] C. Chin, R. Grimm, P. Julienne, and E. Tiesinga. Feshbach resonances in ultracold gases. *Reviews of Modern Physics*, 82(2):1225–1286, 2010. RMP.
- [20] X.-W. Guan, M. T. Batchelor, and C.-H. Lee. Fermi gases in one dimension: from Bethe ansatz to experiments. *Reviews of Modern Physics*, 85(4):1633–1691, 2013.
- [21] L. J. Zhu, M. Garst, A. Rosch, and Q. M. Si. Universally diverging Grüneisen parameter and the magnetocaloric effect close to quantum critical points. *Physical Review Letters*, 91(6), 2003.
- [22] Y. Takahashi and H. Nakano. Magnetovolume effect of itinerant electron ferromagnets. *Journal of Physics: Condensed Matter*, 18(2):521, 2006.
- [23] A. Smith, C. R. H. Bahl, R. Bjrk, K. Engelbrecht, K. K. Nielsen, and N. Pryds. Materials challenges for high performance magnetocaloric refrigeration devices. *Advanced Energy Materials*, 2(11):1288–1318, 2012.
- [24] S. B. Mousumi and P. Pankaj. Study of magnetic entropy and heat capacity in ferrimagnetic Fe_3Se_4 nanorods.

- Journal of Physics D: Applied Physics*, 49(19):195003, 2016.
- [25] O. Breunig, M. Garst, A. Klümper, J. Rohrkamp, M. M. Turnbull, and T. Lorenz. Quantum criticality in the spin-1/2 Heisenberg chain system copper pyrazine dinitrate. *Science Advances*, 3(12):eaao3773, 2017.
 - [26] Z. J. Liu, T. Song, X. W. Sun, Q. Ma, T. Wang, and Y. Guo. Thermal expansion, heat capacity and Grüneisen parameter of iridium phosphide Ir₂P from quasi-harmonic Debye model. *Solid State Communications*, 253:19–23, 2017.
 - [27] K. G. Wilson. The renormalization group: critical phenomena and the Kondo problem. *Review of Modern Physics*, 47:773–840, Oct 1975.
 - [28] See supplemental material.
 - [29] Y.-C. Yu, Y.-Y. Chen, H.-Q. Lin, R. A. Rmer, and X.-W. Guan. Dimensionless ratios: characteristics of quantum liquids and their phase transitions. *Physical Review B*, 94(19):195129, 2016.
 - [30] F. He, Y.-Z. Jiang, Y.-C. Yu, H.-Q. Lin, and X.-W. Guan. Quantum criticality of spinons. *Physical Review B*, 96(22):220401, 2017.
 - [31] L. D. Landau and E. M. Lifshitz. *Statistical Physics: Volume 5*. Butterworth-Heinemann, 1980.
 - [32] F. Weickert, R. Küchler, A. Steppke, L. Pedrero, M. Nicklas, M. Brando, F. Steglich, M. Jaime, V. S. Zapf, A. Paduan-Filho, K. A. Al-Hassanieh, C. D. Batista, and P. Sengupta. Low-temperature thermodynamic properties near the field-induced quantum critical point in NiCl₂-4SC(NH₂)₂. *Physical Review B*, 85(18):184408, 2012.
 - [33] M. Garst and A. Rosch. Sign change of the Grüneisen parameter and magnetocaloric effect near quantum critical points. *Physical Review B*, 72(20), 2005.
 - [34] D. Straß el, P. Kopietz, and S. Eggert. Magnetocaloric effects, quantum critical points, and the Berezinsky-Kosterlitz-Thouless transition in two-dimensional coupled spin-dimer systems. *Physical Review B*, 91(13):134406, 2015.
 - [35] P. Medley, D. M. Weld, H. Miyake, D. E. Pritchard, and W. Ketterle. Spin gradient demagnetization cooling of ultracold atoms. *Physical Review Letters*, 106:195301, May 2011.
 - [36] D. M. Weld, H. Miyake, P. Medley, D. E. Pritchard, and W. Ketterle. Thermometry and refrigeration in a two-component Mott insulator of ultracold atoms. *Physical Review A*, 82:051603, Nov 2010.
 - [37] Y.-Y. Chen, Y.-Z. Jiang, X.-W. Guan, and Q. Zhou. Critical behaviours of contact near phase transitions. *Nature Communications*, 5:5140, 2014.
 - [38] M. Olshanii. Atomic scattering in the presence of an external confinement and a gas of impenetrable Bosons. *Physical Review Letters*, 81(5):938–941, 1998.
 - [39] M. de Souza, P. Menegasso, R. Paupitz, A. Seridonio, and R. E. Lagos. Grüneisen parameter for gases and superfluid helium. *European Journal of Physics*, 37(5), 2016.
 - [40] B. Ekkes. Developments in magnetocaloric refrigeration. *Journal of Physics D: Applied Physics*, 38(23):R381, 2005.
 - [41] V. V. Khovaylo, V. V. Rodionova, S. N. Shevyrtalov, and V. Novosad. Magnetocaloric effect in reduced dimensions: thin films, ribbons, and microwires of Heusler alloys and related compounds. *physica status solidi (b)*, 251(10):2104–2113, 2014.
 - [42] E. H. Lieb and W. Liniger. Exact analysis of an interacting Bose gas. I. The general solution and the ground state. *Physical Review*, 130(4):1605–1616, 1963.
 - [43] V. Dunjko, V. Lorent, and M. Olshanii. Bosons in cigar-shaped traps: Thomas-Fermi regime, Tonks-Girardeau regime, and in between. *Physical Review Letters*, 86(24):5413–5416, 2001.
 - [44] M. Olshanii and V. Dunjko. Short-distance correlation properties of the Lieb-Liniger system and momentum distributions of trapped one-dimensional atomic gases. *Physical Review Letters*, 91(9):090401, 2003.
 - [45] E. H. Lieb and F. Y. Wu. Absence of Mott transition in an exact solution of the short-range, one-band model in one dimension. *Physical Review Letters*, 20(25):1445–1448, 1968.
 - [46] Y.-Y. Chen, G. Watanabe, Y.-C. Yu, X.-W. Guan, and A. del Campo. An interaction-driven many-particle quantum heat engine: universal behavior.
 - [47] W. Niedenzu, I. Mazets, G. Kurizki, and F. Jendrzejewski. Quantized refrigerator for an atomic cloud. *Quantum*, 3:155, jun 2019.
 - [48] C. N. Yang. Some exact results for the many-body problem in one dimension with repulsive delta-function interaction. *Physical Review Letters*, 19(23):1312–1315, 1967.
 - [49] M. Gaudin. Un système a une dimension de fermions en interaction. *Physics Letters A*, 24(1):55–56, jan 1967.
 - [50] G. Orso. Attractive Fermi gases with unequal spin populations in highly elongated traps. *Physical Review Letters*, 98:070402, Feb 2007.
 - [51] H. Hu, X.-J. Liu, and P. D. Drummond. Phase diagram of a strongly interacting polarized Fermi gas in one dimension. *Physical Review Letters*, 98:070403, Feb 2007.
 - [52] M. T. Guan, X. W. Batchelor, C. Lee, and M. Bortz. Phase transitions and pairing signature in strongly attractive Fermi atomic gases. *Physical Review B*, 76:085120, Aug 2007.
 - [53] Y. Liao, A. S. C. Rittner, T. Paprotta, W. Li, G. B. Partridge, R. G. Hulet, S. K. Baur, and E. J. Mueller. Spin-imbalance in a one-dimensional Fermi gas. *Nature*, 467:567, 2010.
 - [54] X.-W. Guan and T.-L. Ho. Quantum criticality of a one-dimensional attractive Fermi gas. *Physical Review A*, 84(2):023616, 2011.
 - [55] M. P. A. Fisher, P. B. Weichman, G. Grinstein, and D. S. Fisher. Boson localization and the superfluid-insulator transition. *Physical Review B*, 40(1):546–570, 1989.
 - [56] Y.-Z. Jiang, Y.-Y. Chen, and X.-W. Guan. Understanding many-body physics in one dimension from the Lieb-Liniger model. *Chinese Physics B*, 24(5):050311, 2015.
 - [57] S. Cheng, Y.-C. Yu, M. T. Batchelor, and X.-W. Guan. Fulde-Ferrell-Larkin-Ovchinnikov correlation and free fluids in the one-dimensional attractive Hubbard model. *Physical Review B*, 97(12):121111, 2018. PRB.
 - [58] S. Sachdev. *Quantum Phase Transitions*. Cambridge University Press, Cambridge, 2001.
 - [59] C. H. Lee and C. K. Gan. Anharmonic interatomic force constants and thermal conductivity from Grüneisen parameters: an application to graphene. *Physical Review B*, 96(3), 2017.
 - [60] S. Watanabe and K. Miyake. Grüneisen parameter and thermal expansion by the self-consistent renormalization theory of spin fluctuations. *Journal of the Physical Soci-*

- ety of Japan*, 87(3):034712, 2018.
- [61] H. Pethick, C. J. Smith. *Bose-Einstein Condensation in Dilute Gases*. Cambridge University Press, Cambridge, 2 edition, 2008.
 - [62] C. N. Yang and C. P. Yang. Thermodynamics of a one-dimensional system of Bosons with repulsive delta-function interaction. *Journal of Mathematical Physics*, 10(7):1115–1122, 1969.
 - [63] Here we do not write out explicitly the vertical lines and corresponding variables in the partial derivatives, where the derivatives are calculated in the grand canonical ensemble with variables V (volume), T (temperature), H (magnetic field), and c (coupling strength).
 - [64] L. Peng, Y.-C. Yu and X.-W. Guan, in preparation, 2019.

Yi-Cong Yu, Shi-Zhong Zhang and Xi-Wen Gaun

1. THE DEFINITION OF THE GRÜNEISEN PARAMETER

In the microscopic point of view the Grüneisen parameter is related to the derivation of the model frequency and the bulk volume. The most simple consideration about the thermodynamic quantities in solid state physics is the Einstein model, where the excitation in a solid is described by N phonon with the same frequency ω_0 , or equivalently saying, the solid is composed by N independent harmonic oscillator with the spectrum $E_n = (n + \frac{1}{2})\hbar\omega_0$. The partition function is

$$\log Z = Nf(\hbar\omega_0\beta), \quad (\text{S1})$$

where β is defined by $\beta = 1/(k_B T)$ with the Boltzmann constant k_B , and the analytic function $f(x)$ is defined by $f(x) = \frac{1}{2}x - \log(e^x - 1)$. It is obvious that in Einstein model the temperature T and the frequency of the phonon ω_0 are homogeneous in partition function Z and in the entropy

$$\begin{aligned} S &= k_B(\log Z - \beta \frac{\partial \log Z}{\partial \beta}) \\ &= Nk_B[f(\hbar\omega_0\beta) - \hbar\omega_0\beta f'(\hbar\omega_0\beta)]. \end{aligned} \quad (\text{S2})$$

Although the energy $E = -\frac{\partial}{\partial \beta} \log Z$ loses the homogeneity for T and ω_0 , the specific heat

$$C_V = \frac{\partial E}{\partial T} = k_B \beta^2 \frac{\partial^2}{\partial \beta^2} \log Z$$

The analysis above implies that the Grüneisen parameter is closely related to the homogeneity of the thermodynamic quantities, thus it can be easily extended to the Deby model, in which a solid is described by independent phonons with different frequencies. In this case the partition function:

$$\log Z = \sum_i N_i f(\hbar\omega_i\beta), \quad (\text{S7})$$

where the ω_i presents the i -th vibrational frequency in the solid. Similarly, we have:

$$\begin{aligned} C_V &= \sum_i N_i k_B [(\hbar\omega_i\beta)^2 f''(\hbar\omega_i\beta)], \\ V \frac{\partial S}{\partial V} &= \sum_i N_i V \frac{\partial S}{\partial \omega_i} \frac{\partial \omega_i}{\partial V} \end{aligned} \quad (\text{S8})$$

$$= Nk_B [(\hbar\omega_0\beta)^2 f''(\hbar\omega_0\beta)] \quad (\text{S3})$$

is again homogeneous, and the same for

$$\omega_0 \frac{\partial S}{\partial \omega_0} = -Nk_B [(\hbar\omega_0\beta)^2 f''(\hbar\omega_0\beta)]. \quad (\text{S4})$$

In fact these two quantities have the simple relation $\omega_0 \frac{\partial S}{\partial \omega_0} = -C_V$. Because the frequency of the phonon is decided by the size of the solid, we have the relation:

$$C_V = -\omega_0 \frac{\partial S}{\partial \omega_0} = -\frac{\omega_0}{V} \frac{\partial V}{\partial \omega_0} (V \frac{\partial S}{\partial V}), \quad (\text{S5})$$

if we define $\Gamma^{-1} = -\frac{\omega_0}{V} \frac{\partial V}{\partial \omega_0}$, then according to equation (S5) we have

$$\Gamma = \frac{V \frac{\partial S}{\partial V}}{C_V}. \quad (\text{S6})$$

This definition is from the original research of E. Grüneisen when he was studying the Einstein model [1, 2]. Notice that although the system is described by the frequency of the phonon which is a microscopic quantity, the definition (1) in the main text implies that the relationship between ω_0 and V can be related to some observable thermodynamic quantity.

$$= \sum_i -(\frac{V}{\omega_i} \frac{\partial \omega_i}{\partial V}) N_i k_B [(\hbar\omega_i\beta)^2 f''(\hbar\omega_i\beta)], \quad (\text{S9})$$

where the ω_i presents the i -th vibrational frequency in the solid, and for every ω_i the specific heat and the $\omega_i \frac{\partial S}{\partial \omega_i}$ is related as equation (S5). If we define the Grüneisen parameter for i -th frequency

$$\Gamma_i = -\frac{d \log \omega_i}{d \log V}, \quad (\text{S10})$$

we finally obtain the total Grüneisen parameter by the Γ_i and $C_{V,i}$ for each mode

$$\Gamma = \frac{\sum_i \Gamma_i C_{V,i}}{\sum_i C_{V,i}}. \quad (\text{S11})$$

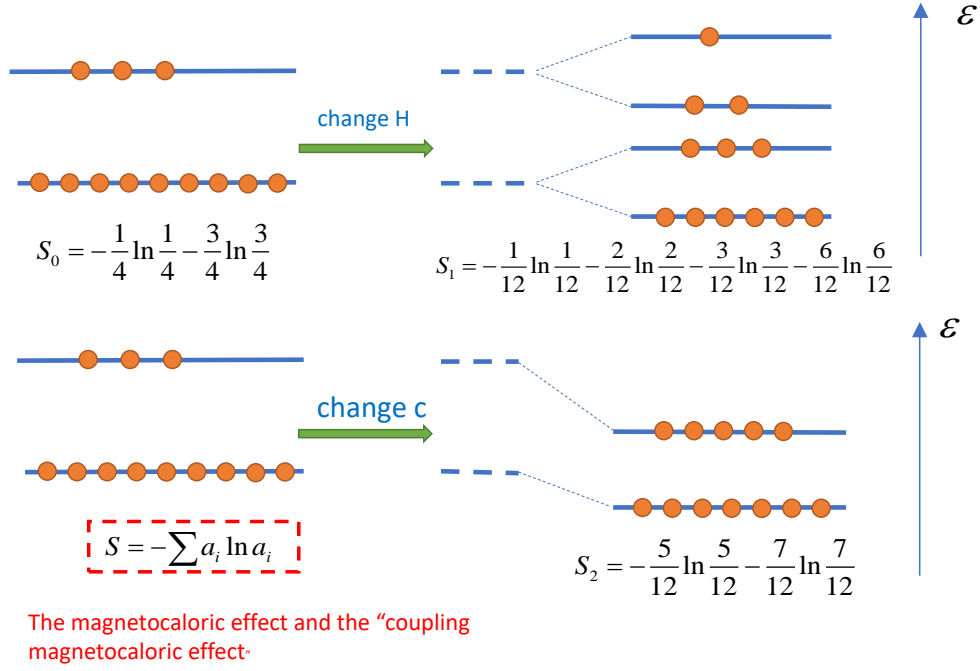


FIG. S1: A diagrammatic illustration of the magnetocaloric and interaction driven magnetocaloric effects for a system of 12 particles. A change of the magnetic field (upper panel) or a variation of interaction strength (lower panel) essentially influences the spectral structures of the quantum many-body system. The former leads to the changes of particle distribution among energy levels, whereas the later may cause energy level distribution changed, so that the entropies $S_{1,2}$ for the two configures are respectively changed.

2. THE PROOF OF THE IDENTITY FOR GRÜNEISEN PARAMETERS

We give a brief proof of the identity (13) by general statistic approach. We begin with the partition function of the grand canonical ensemble

$$Z = \sum_{n,m} e^{-\alpha n - \beta \epsilon_{n,m}} \quad (\text{S12})$$

where the $\epsilon_{n,m}$ presents the energy of the m th energy level of n particle Hamiltonian, β is the inversed temperature $\beta = 1/(k_B T)$, and $\alpha = -\beta\mu$ with chemical potential μ . The population function is

$$a_{n,m} = \frac{1}{Z} e^{-\alpha n - \beta \epsilon_{n,m}} \quad (\text{S13})$$

and the entropy is

$$S = - \sum_{n,m} a_{n,m} \ln a_{n,m} \quad (\text{S14})$$

Now for every function $f_{n,m}$ of the quantum index n, m , we can define the expectation $\langle f_{n,m} \rangle$ by

$$\langle f_{n,m} \rangle = \sum_{n,m} a_{n,m} f_{n,m} \quad (\text{S15})$$

obviously we have $N = \langle n \rangle$ for the particle number, $E = \langle \epsilon_{n,m} \rangle$ for the internal energy, and $p = -\langle \frac{\partial \epsilon_{n,m}}{\partial V} \rangle$ for the pressure. From the definition eq. (S12) and eq. (S13) we immediately obtain

$$\begin{aligned} \frac{\partial a_{n,m}}{\partial \alpha} &= a_{n,m} \cdot (\langle n \rangle - n) \\ \frac{\partial a_{n,m}}{\partial \beta} &= a_{n,m} \cdot (\langle \epsilon_{n,m} \rangle - \epsilon_{n,m}) \\ \frac{\partial a_{n,m}}{\partial y} &= a_{n,m} \cdot (\langle \frac{\partial \epsilon_{n,m}}{\partial y} \rangle - \frac{\partial \epsilon_{n,m}}{\partial y}) \end{aligned} \quad (\text{S16})$$

here y presents any external field, it can be volume, magnetic field or the coupling, i.e. $y = V, H, c$, next we introduce the covariance of two function $f_{n,m}, g_{n,m}$ as

$$\text{Cov}(F, G) = \sum_{n,m} a_{n,m} f_{n,m} g_{n,m} - \langle f_{n,m} \rangle \langle g_{n,m} \rangle \quad (\text{S17})$$

here the $f_{n,m}$ and $g_{n,m}$ is the value of thermodynamic quantities F and G in the state $a_{n,m}$ respectively. Apply this notation and use eqs. (S12), (S13) and (S16) we have

$$\begin{aligned} dS &= [\beta \text{Cov}(E, N) + \alpha \text{Cov}(N, N)] d\alpha \\ &+ [\beta \text{Cov}(E, E) + \alpha \text{Cov}(E, N)] d\beta \\ &+ \beta [\beta \text{Cov}(E, \frac{\partial E}{\partial V}) + \alpha \text{Cov}(N, \frac{\partial E}{\partial V})] dV \\ &+ \beta [\beta \text{Cov}(E, \frac{\partial E}{\partial H}) + \alpha \text{Cov}(N, \frac{\partial E}{\partial H})] dH \end{aligned}$$

$$\begin{aligned}
& +\beta[\beta\text{Cov}(E, \frac{\partial E}{\partial c}) + \alpha\text{Cov}(N, \frac{\partial E}{\partial c})]dc \\
dE &= \text{Cov}(E, N)d\alpha + \text{Cov}(E, E)d\beta \\
& +[\frac{\partial E}{\partial V} + \beta\text{Cov}(E, \frac{\partial E}{\partial V})]dV \\
& +[\frac{\partial E}{\partial H} + \beta\text{Cov}(E, \frac{\partial E}{\partial H})]dH \\
& +[\frac{\partial E}{\partial c} + \beta\text{Cov}(E, \frac{\partial E}{\partial c})]dc \\
dN &= \text{Cov}(N, N)d\alpha + \text{Cov}(E, N)d\beta + \beta\text{Cov}(N, \frac{\partial E}{\partial V})dV \\
& +\beta\text{Cov}(N, \frac{\partial E}{\partial H})dH + \beta\text{Cov}(N, \frac{\partial E}{\partial c})dc \quad (\text{S18})
\end{aligned}$$

Apply the (S18) we can get the thermodynamic quantities

$$\begin{aligned}
\frac{\partial S}{\partial \beta} |_{N,V,H,c} &= \beta[\text{Cov}(E, E) - \frac{\text{Cov}(E, N)\text{Cov}(E, N)}{\text{Cov}(N, N)}] \\
\frac{\partial S}{\partial V} |_{N,\beta,H,c} &= \beta^2[\text{Cov}(E, \frac{\partial E}{\partial V}) - \frac{\text{Cov}(E, N)\text{Cov}(N, \frac{\partial E}{\partial V})}{\text{Cov}(N, N)}] \\
\frac{\partial S}{\partial H} |_{N,\beta,V,c} &= \beta^2[\text{Cov}(E, \frac{\partial E}{\partial H}) - \frac{\text{Cov}(E, N)\text{Cov}(N, \frac{\partial E}{\partial H})}{\text{Cov}(N, N)}] \\
\frac{\partial S}{\partial c} |_{N,\beta,V,H} &= \beta^2[\text{Cov}(E, \frac{\partial E}{\partial c}) - \frac{\text{Cov}(E, N)\text{Cov}(N, \frac{\partial E}{\partial c})}{\text{Cov}(N, N)}] \quad (\text{S19})
\end{aligned}$$

Suppose the scaling behaviour of the spectrum: $L \rightarrow e^\lambda L$, $c \rightarrow e^{-\lambda} c$, $H \rightarrow e^{-2\lambda} H$, $\epsilon_{n,m} \rightarrow e^{-2\lambda} \epsilon_{n,m}$, or in other words the spectrums have the homogenous form $\epsilon_{n,m}(L, H, c) = L^{-2} f_{n,m}(L^2 H, Lc)$ where the $f_{n,m}$ are analytical functions. We thus have the identity:

$$L \frac{\partial \epsilon_{n,m}}{\partial L} = -2\epsilon_{n,m} + 2H \frac{\partial \epsilon_{n,m}}{\partial H} + c \frac{\partial \epsilon_{n,m}}{\partial c} \quad (\text{S20})$$

notice $\beta \frac{\partial S}{\partial \beta} = -T \frac{\partial S}{\partial T}$ and $L \frac{\partial \epsilon_{n,m}}{\partial L} = d \cdot V \frac{\partial \epsilon_{n,m}}{\partial V}$ where the d is the dimension of the system, and notice that the $\mathbf{Cov}(F, G)$ is bilinear, then substitute eq. (S20) into (S19) we arrive

$$d \cdot V \frac{\partial S}{\partial V} = 2T \frac{\partial S}{\partial T} + 2H \frac{\partial S}{\partial H} + c \frac{\partial S}{\partial c} \quad (\text{S21})$$

substitute the definitions of GPs

$$\Gamma = \frac{V \frac{\partial S}{\partial V}}{C_V}, \quad (\text{S22})$$

$$\Gamma_{\text{mag}} = -\frac{H \frac{\partial S}{\partial H} |_{N,T,V}}{T \frac{\partial S}{\partial T} |_{N,B,V}}, \quad (\text{S23})$$

$$\Gamma_{\text{int}} = -\frac{c \frac{\partial S}{\partial c} |_{N,H,T,V}}{T \frac{\partial S}{\partial T} |_{N,H,c,V}} \quad (\text{S24})$$

into (S21), we prove the identity

$$d \cdot \Gamma + 2\Gamma_{\text{mag}} + \Gamma_{\text{coupling}} = 2. \quad (\text{S25})$$

The spectral structures of quantum gases are sensitive to system volume, external fields and interactions, see Fig. S1. This identity quantifies universal scalings of the GPs in quantum systems of ultracold atoms in all dimensions.

3. THE BETHE ANSATZ SOLUTIONS FOR LIEB-LINIGER MODEL

The first quantized form of the Lieb-Liniger Hamiltonian is [42]

$$\hat{H} = -\sum_{i=1}^N \frac{\partial^2}{\partial x_i^2} + 2c \sum_{i>j} \delta(x_i - x_j) \quad (\text{S26})$$

The dimensionless interaction strength is defined by $\gamma = c/n$ with $c = -2/a_{1D}$, where $n = N/L$ is the linear density. The interaction strength can be controlled by tuning either ω_\perp or a_s in experiments. Here we set Boltzmann constant $k_B = 1$, $2m = \hbar = 1$.

We consider $c > 0$ for repulsive interaction. The Bethe Ansatz equation for the ground state is given in term of the quasimomentum distribution $\rho\{k\}$

$$\rho(k) = \frac{1}{2\pi} + \frac{1}{2\pi} \int_{-k_F}^{k_F} \frac{2c}{c^2 + (k-q)^2} \rho(q) dq \quad (\text{S27})$$

Where k_F is the cut-off momentum, i.e. Fermi-like momentum. The particle density is given by $n = \int_{-k_F}^{k_F} \rho(k) dk$. The ground state energy can be expressed as

$$E = Nn^2 \int_{-k_F}^{k_F} \rho(k) k^2 dk \quad (\text{S28})$$

In describing the thermodynamics of the model the key quantity is the dressed energy

$$\epsilon(k) = T \ln(\rho^h(k)/\rho(k)) \quad (\text{S29})$$

which plays the role of excitation energy measured from the energy level $\epsilon(k_F) = 0$. The thermodynamics of the model in equilibrium follows from the Yang-Yang equation [62]

$$\epsilon(k) = \epsilon^0(k) - \mu - T \int_{-\infty}^{\infty} dq a_2(k-q) \ln(1 + e^{-\epsilon(q)/T}) \quad (\text{S30})$$

where $\epsilon^0(k) = \frac{\hbar^2}{2m} k^2$ is the bare dispersion, μ is the chemical potential and the integration kernel is denoted as $a_2(x) = \frac{1}{2\pi} \frac{2c}{c^2 + x^2}$ is the integration kernel.

The pressure $p(T)$ is given in terms of the dressed energy by

$$p(T) = \frac{T}{2\pi} \int_{-\infty}^{\infty} dk \ln(1 + e^{-\epsilon(k)/T}). \quad (\text{S31})$$

and the grand potential is $\Omega(\mu, T, c) = -pL$, then all the equilibrium thermodynamic quantities can be obtained by differential of Ω .

4. THE BETHE ANSATZ SOLUTIONS FOR THE YANG-GAUDIN MODEL

We consider the Yang-Gaudin model [48, 49], which describes a 1D of the N δ -interacting spin- $\frac{1}{2}$ fermions. It is constrained by periodic boundary conditions to a line of length L and subject to an external magnetic field H . The Hamiltonian reads

$$\hat{H} = - \sum_{i=1}^N \frac{\partial^2}{\partial x_i^2} + 2c \sum_{i < j}^N \delta(x_i - x_j). \quad (\text{S32})$$

The BA equations are

$$\begin{aligned} \exp(ik_j L) &= \prod_{\alpha=1}^M \frac{k_j - \Lambda_\alpha + ic/2}{k_j - \Lambda_\alpha - ic/2}, \\ \prod_{j=1}^N \frac{\Lambda_\alpha - k_j + ic/2}{\Lambda_\alpha - k_j - ic/2} &= - \prod_{\beta=1}^M \frac{\Lambda_\alpha - \Lambda_\beta + ic}{\Lambda_\alpha - \Lambda_\beta - ic}. \end{aligned} \quad (\text{S33})$$

According to the Yang-Yang method, we can derive the TBA equations of the attractive Yang-Gaudin model [20]:

$$\begin{aligned} \epsilon^b(k) &= 2(k^2 - \mu - \frac{1}{4}c^2) + Ta_2 * \ln(1 + e^{\epsilon^b(k)/T}) \\ &\quad + Ta_1 * \ln(1 + e^{\epsilon^u(k)/T}), \\ \epsilon^u(k) &= k^2 - \mu - \frac{1}{2}H + Ta_1 * \ln(1 + e^{\epsilon^b(k)/T}) \\ &\quad - T \sum_{l=1}^{\infty} a_l * \ln(1 + \eta^{-1}(k)), \\ \ln \eta_l(\lambda) &= \frac{lH}{T} + a_l * \ln(1 + e^{-\epsilon^u(k)/T}) \\ &\quad + \sum_{m=1}^{\infty} T_{lm} * \ln(1 + \eta_m^{-1}(\lambda)) \end{aligned} \quad (\text{S34})$$

The pressure in terms of these finite temperature dressed energies is given by

$$\begin{aligned} p &= \frac{T}{\pi} \int_{-\infty}^{\infty} dk \ln(1 + e^{-\epsilon^b(k)/T}) \\ &\quad + \frac{T}{2\pi} \int_{-\infty}^{\infty} dk \ln(1 + e^{-\epsilon^u(k)/T}). \end{aligned} \quad (\text{S35})$$

Note that in the TBAE for Gaudin-Yang model (S34) there are "strings" $\eta_l(\lambda)$ which present the excitation of spin flipping. In the low temperature limit where $H/T \gg 1$, the contributions of strings to the thermodynamic potentials are restrained, then we can ignore the strings and simplify the TBAE

$$\begin{aligned} \epsilon^b(k) &= 2(k^2 - \mu - \frac{1}{4}c^2) + Ta_2 * \ln(1 + e^{\epsilon^b(k)/T}) \\ &\quad + Ta_1 * \ln(1 + e^{\epsilon^u(k)/T}), \\ \epsilon^u(k) &= k^2 - \mu - \frac{1}{2}H + Ta_1 * \ln(1 + e^{\epsilon^b(k)/T}). \end{aligned} \quad (\text{S36})$$

and in the strong coupling limit $c \gg 1$, applying the method similar to the Bose gas case, we have

$$\begin{aligned} \epsilon^{(u)}(k) &= D_1 \cdot k^2 - \mu - \frac{1}{2}H + \frac{2}{|c|} p^{(b)} \\ &\quad + \frac{2}{\sqrt{2\pi}|c|^3} T^{5/2} \text{Li}_{\frac{5}{2}}(-e^{A_0^{(b)}/T}), \\ \epsilon^{(b)}(k) &= D_2 \cdot 2k^2 - 2\mu - \frac{1}{2}c^2 + \frac{4}{|c|} p^{(u)} + \frac{1}{|c|} p^{(b)} \\ &\quad + \frac{4\sqrt{2}T^{5/2}}{\sqrt{2\pi}|c|^3} \text{Li}_{\frac{5}{2}}(-e^{A_0^{(u)}/T}) \\ &\quad + \frac{T^{5/2}}{4\sqrt{2\pi}|c|^3} \text{Li}_{\frac{5}{2}}(-e^{A_0^{(b)}/T}). \end{aligned} \quad (\text{S37})$$

with the $D_{1,2}$ the correction of the quadratic terms

$$\begin{aligned} D_1 &= 1 - \frac{8}{|c|^3} p^{(2)}, \\ D_2 &= 1 - \frac{8}{|c|^3} p^{(1)} - \frac{1}{2|c|^3} p^{(2)}. \end{aligned} \quad (\text{S38})$$

We argue that these corrections do not contribute as we only consider the first three terms of the series in the thermodynamic quantities. The analytical equations for the Gaudin-Yang model is

$$\begin{aligned} p^{(r)} &= - \frac{\sqrt{r}}{2\sqrt{\pi}} T^{\frac{3}{2}} \text{Li}_{\frac{3}{2}}(-e^{A^{(r)}/T}), \\ A^{(r)} &= A_0^{(r)} - \sum_{m=1}^N D_{rm} \frac{p^{(m)}}{|c|} \end{aligned} \quad (\text{S39})$$

where $r = 1, 2$ is the index for unpaired and paired fermions, $A_0^{(1)} = \mu + H/2$ and $A_0^{(2)} = 2\mu + c^2/2$, and the D_{rm} is the matrix $D_{11} = 0, D_{12} = 2, D_{21} = 4, D_{22} = 1$. Next we normalize equation (S39) by the binding energy $\epsilon = c^2/2$, define

$$\begin{aligned} \tilde{p}^{(r)} &= \frac{p^{(r)}}{\frac{1}{2}|c|^3}, \quad \tilde{A}^{(r)} = \frac{A^{(r)}}{\frac{1}{2}|c|^2}, \quad \tilde{\mu} = \frac{\mu}{\frac{1}{2}|c|^2}, \\ h &= \frac{H}{\frac{1}{2}|c|^2}, \quad t = \frac{T}{\frac{1}{2}|c|^2}. \end{aligned} \quad (\text{S40})$$

then the equation (S39) becomes

$$\begin{aligned} \tilde{p}^{(r)} &= - \frac{\sqrt{r}}{2\sqrt{2\pi}} t^{\frac{3}{2}} \text{Li}_{\frac{3}{2}}(-e^{\tilde{A}^{(r)}/t}), \\ \tilde{A}^{(r)} &= \tilde{A}_0^{(r)} - \sum_{m=1}^N D_{rm} \tilde{p}^{(m)}, \end{aligned} \quad (\text{S41})$$

where $\tilde{A}_0^{(1)} = \tilde{\mu} + h/2$, $\tilde{A}_0^{(2)} = 2\tilde{\mu} + 1$. Then up to the first three terms the result of the pressures are

$$\tilde{p}^{(1)} = - \frac{1}{2\sqrt{2\pi}} t^{\frac{3}{2}} \text{Li}_{\frac{3}{2}}(-e^{\tilde{A}^{(1)}/t}), \quad (\text{S42})$$

$$\tilde{p}^{(2)} = -\frac{1}{2\sqrt{\pi}} t^{\frac{3}{2}} \text{Li}_{\frac{3}{2}}(-e^{\tilde{A}^{(2)}/t}), \quad (\text{S43})$$

$$\tilde{A}^{(1)} = \tilde{A}_0^{(1)} + \frac{f_{\frac{3}{2}}^{(2)}}{\sqrt{\pi}} + \frac{\sqrt{2}f_{\frac{3}{2}}^{(1)}f_{\frac{1}{2}}^{(2)}}{\pi} + \frac{f_{\frac{1}{2}}^{(2)}f_{\frac{3}{2}}^{(2)}}{2\pi}, \quad (\text{S44})$$

$$\tilde{A}^{(2)} = \tilde{A}_0^{(2)} + \frac{\sqrt{2}f_{\frac{3}{2}}^{(1)}}{\sqrt{\pi}} + \frac{f_{\frac{3}{2}}^{(2)}}{2\sqrt{\pi}} + \frac{f_{\frac{3}{2}}^{(1)}f_{\frac{1}{2}}^{(2)}}{\sqrt{2\pi}}$$

$$+ \frac{\sqrt{2}f_{\frac{1}{2}}^{(1)}f_{\frac{3}{2}}^{(2)}}{\pi} + \frac{f_{\frac{1}{2}}^{(2)}f_{\frac{3}{2}}^{(2)}}{4\pi}. \quad (\text{S45})$$

Here the definition $f_s^{(r)} \triangleq t^s \text{Li}_s(-e^{\tilde{A}_0^{(r)}/t})$, $r = 1, 2$. And for further discussions, we list the result of all the first and higher order partial derivatives of the pressure

$$\tilde{n} = \frac{n}{|c|} = \frac{\partial \tilde{p}}{\partial \tilde{\mu}} = -\frac{F_{\frac{1}{2}}^{(1)}}{2\sqrt{2\pi}} - \frac{F_{\frac{1}{2}}^{(2)}}{\sqrt{\pi}} - \frac{\sqrt{2}F_{\frac{1}{2}}^{(1)}F_{\frac{1}{2}}^{(2)}}{\pi} - \frac{(F_{\frac{1}{2}}^{(2)})^2}{2\pi} - \frac{(F_{\frac{1}{2}}^{(1)})^2F_{\frac{1}{2}}^{(2)}}{2\pi^{3/2}} - \frac{3F_{\frac{1}{2}}^{(1)}(F_{\frac{1}{2}}^{(2)})^2}{\sqrt{2}\pi^{3/2}} - \frac{(F_{\frac{1}{2}}^{(2)})^3}{4\pi^{3/2}}, \quad (\text{S46})$$

$$\tilde{m} = \frac{m}{|c|} = \frac{\partial \tilde{p}}{\partial h} = -\frac{F_{\frac{1}{2}}^{(1)}}{4\sqrt{2\pi}} - \frac{F_{\frac{1}{2}}^{(1)}F_{\frac{1}{2}}^{(2)}}{2\sqrt{2\pi}} - \frac{(F_{\frac{1}{2}}^{(1)})^2F_{\frac{1}{2}}^{(2)}}{4\pi^{3/2}} - \frac{F_{\frac{1}{2}}^{(1)}(F_{\frac{1}{2}}^{(2)})^2}{4\sqrt{2}\pi^{3/2}}, \quad (\text{S47})$$

$$\tilde{\kappa} = \frac{\epsilon^b}{|c|} \kappa = \frac{\partial^2 \tilde{p}}{\partial \tilde{\mu}^2} = -\frac{F_{-\frac{1}{2}}^{(1)}}{2\sqrt{2\pi}} - \frac{2F_{-\frac{1}{2}}^{(2)}}{\sqrt{\pi}} - \frac{3\sqrt{2}F_{\frac{1}{2}}^{(1)}F_{-\frac{1}{2}}^{(2)}}{\pi} - \frac{3F_{-\frac{1}{2}}^{(1)}F_{\frac{1}{2}}^{(2)}}{\sqrt{2\pi}} - \frac{3F_{-\frac{1}{2}}^{(2)}F_{\frac{1}{2}}^{(2)}}{\pi} \\ - \frac{3F_{\frac{1}{2}}^{(1)}F_{\frac{1}{2}}^{(1)}F_{-\frac{1}{2}}^{(2)}}{\pi^{3/2}} - \frac{3F_{-\frac{1}{2}}^{(1)}F_{\frac{1}{2}}^{(1)}F_{\frac{1}{2}}^{(2)}}{2\pi^{3/2}} - \frac{21F_{\frac{1}{2}}^{(1)}F_{-\frac{1}{2}}^{(2)}F_{\frac{1}{2}}^{(2)}}{\sqrt{2}\pi^{3/2}} - \frac{15F_{-\frac{1}{2}}^{(1)}F_{\frac{1}{2}}^{(2)}F_{\frac{1}{2}}^{(2)}}{2\sqrt{2}\pi^{3/2}} - \frac{3F_{-\frac{1}{2}}^{(2)}F_{\frac{1}{2}}^{(2)}F_{\frac{1}{2}}^{(2)}}{\pi^{3/2}}, \quad (\text{S48})$$

$$\tilde{\chi} = \frac{\epsilon^b}{|c|} \chi = \frac{\partial^2 \tilde{p}}{\partial h^2} = -\frac{F_{-\frac{1}{2}}^{(1)}}{8\sqrt{2\pi}} - \frac{F_{-\frac{1}{2}}^{(1)}F_{\frac{1}{2}}^{(2)}}{4\sqrt{2\pi}} - \frac{F_{\frac{1}{2}}^{(1)}F_{\frac{1}{2}}^{(1)}F_{-\frac{1}{2}}^{(2)}}{4\pi^{3/2}} - \frac{3F_{-\frac{1}{2}}^{(1)}F_{\frac{1}{2}}^{(1)}F_{\frac{1}{2}}^{(2)}}{8\pi^{3/2}} - \frac{F_{-\frac{1}{2}}^{(1)}F_{\frac{1}{2}}^{(2)}F_{\frac{1}{2}}^{(2)}}{8\sqrt{2}\pi^{3/2}}, \quad (\text{S49})$$

$$\tilde{s} = \frac{\tilde{S}}{L} = \frac{\partial \tilde{p}}{\partial t} = \frac{S}{L|c|} = -\frac{3}{4\sqrt{2\pi}} \frac{F_{\frac{3}{2}}^{(1)}}{t} - \frac{3}{4\sqrt{\pi}} \frac{F_{\frac{3}{2}}^{(2)}}{t} + \frac{1}{2\sqrt{2\pi}} \frac{\tilde{A}^{(1)}F_{\frac{1}{2}}^{(1)}}{t} + \frac{1}{2\sqrt{\pi}} \frac{\tilde{A}^{(2)}F_{\frac{1}{2}}^{(2)}}{t} \\ - \frac{3F_{\frac{3}{2}}^{(1)}F_{\frac{1}{2}}^{(2)}}{2\sqrt{2}\pi t} - \frac{3F_{\frac{1}{2}}^{(1)}F_{\frac{3}{2}}^{(2)}}{4\sqrt{2}\pi t} - \frac{3F_{\frac{1}{2}}^{(2)}F_{\frac{3}{2}}^{(2)}}{8\pi t} + \frac{\tilde{A}^{(1)}F_{\frac{1}{2}}^{(1)}F_{\frac{1}{2}}^{(2)}}{\sqrt{2}\pi t} + \frac{\tilde{A}^{(2)}F_{\frac{1}{2}}^{(1)}F_{\frac{1}{2}}^{(2)}}{2\sqrt{2}\pi t} + \frac{\tilde{A}^{(2)}F_{\frac{1}{2}}^{(2)}F_{\frac{1}{2}}^{(2)}}{4\pi t} \\ - \frac{3F_{\frac{1}{2}}^{(1)}F_{\frac{1}{2}}^{(1)}F_{\frac{1}{2}}^{(2)}}{4\pi^{3/2}t} - \frac{3F_{\frac{1}{2}}^{(1)}F_{\frac{1}{2}}^{(2)}F_{\frac{1}{2}}^{(2)}}{4\sqrt{2}\pi^{3/2}t} - \frac{15F_{\frac{1}{2}}^{(1)}F_{\frac{1}{2}}^{(2)}F_{\frac{3}{2}}^{(2)}}{8\sqrt{2}\pi^{3/2}t} - \frac{3F_{\frac{1}{2}}^{(2)}F_{\frac{1}{2}}^{(2)}F_{\frac{3}{2}}^{(2)}}{16\pi^{3/2}t} + \frac{\tilde{A}^{(1)}F_{\frac{1}{2}}^{(1)}F_{\frac{1}{2}}^{(1)}F_{\frac{1}{2}}^{(2)}}{2\pi^{3/2}t} \\ + \frac{\tilde{A}^{(1)}F_{\frac{1}{2}}^{(1)}F_{\frac{1}{2}}^{(2)}F_{\frac{1}{2}}^{(2)}}{2\sqrt{2}\pi^{3/2}t} + \frac{5\tilde{A}^{(2)}F_{\frac{1}{2}}^{(1)}F_{\frac{1}{2}}^{(2)}F_{\frac{1}{2}}^{(2)}}{4\sqrt{2}\pi^{3/2}t} + \frac{\tilde{A}^{(2)}F_{\frac{1}{2}}^{(2)}F_{\frac{1}{2}}^{(2)}F_{\frac{1}{2}}^{(2)}}{8\pi^{3/2}t}, \quad (\text{S50})$$

$$\frac{\tilde{c}_V}{t} = \frac{c_V}{T} \frac{\epsilon^b}{|c|} = \frac{\partial^2 \tilde{p}}{\partial t^2} \\ = -\frac{(\tilde{A}^{(1)})^2F_{-\frac{1}{2}}^{(1)}}{2\sqrt{2}\pi t^2} + \frac{\tilde{A}^{(1)}F_{\frac{1}{2}}^{(1)}}{2\sqrt{2}\pi t^2} - \frac{3F_{\frac{3}{2}}^{(1)}}{8\sqrt{2}\pi t^2} - \frac{(\tilde{A}^{(2)})^2F_{-\frac{1}{2}}^{(2)}}{2\sqrt{\pi}t^2} + \frac{\tilde{A}^{(2)}F_{\frac{1}{2}}^{(2)}}{2\sqrt{\pi}t^2} - \frac{3F_{\frac{3}{2}}^{(2)}}{8\sqrt{\pi}t^2} \\ - \frac{\sqrt{2}\tilde{A}^{(1)}\tilde{A}^{(2)}F_{\frac{1}{2}}^{(1)}F_{-\frac{1}{2}}^{(2)}}{\pi t^2} - \frac{(\tilde{A}^{(2)})^2F_{\frac{1}{2}}^{(1)}F_{-\frac{1}{2}}^{(2)}}{2\sqrt{2}\pi t^2} + \frac{3\tilde{A}^{(2)}F_{\frac{3}{2}}^{(1)}F_{-\frac{1}{2}}^{(2)}}{\sqrt{2}\pi t^2} - \frac{(\tilde{A}^{(1)})^2F_{-\frac{1}{2}}^{(1)}F_{\frac{1}{2}}^{(2)}}{\sqrt{2}\pi t^2} \\ - \frac{\tilde{A}^{(1)}\tilde{A}^{(2)}F_{-\frac{1}{2}}^{(1)}F_{\frac{1}{2}}^{(2)}}{\sqrt{2}\pi t^2} + \frac{\sqrt{2}\tilde{A}^{(1)}F_{\frac{1}{2}}^{(1)}F_{\frac{1}{2}}^{(2)}}{\pi t^2} + \frac{\tilde{A}^{(2)}F_{\frac{1}{2}}^{(1)}F_{\frac{1}{2}}^{(2)}}{\sqrt{2}\pi t^2} - \frac{9F_{\frac{3}{2}}^{(1)}F_{\frac{1}{2}}^{(2)}}{4\sqrt{2}\pi t^2} \\ - \frac{3(\tilde{A}^{(2)})^2F_{-\frac{1}{2}}^{(2)}F_{\frac{1}{2}}^{(2)}}{4\pi t^2} + \frac{\tilde{A}^{(2)}F_{\frac{1}{2}}^{(2)}F_{\frac{1}{2}}^{(2)}}{2\pi t^2} + \frac{3\tilde{A}^{(1)}F_{-\frac{1}{2}}^{(1)}F_{\frac{3}{2}}^{(2)}}{2\sqrt{2}\pi t^2} - \frac{9F_{\frac{1}{2}}^{(1)}F_{\frac{3}{2}}^{(2)}}{8\sqrt{2}\pi t^2} \\ + \frac{3\tilde{A}^{(2)}F_{-\frac{1}{2}}^{(2)}F_{\frac{3}{2}}^{(2)}}{4\pi t^2} - \frac{9F_{\frac{1}{2}}^{(2)}F_{\frac{3}{2}}^{(2)}}{16\pi t^2} - \frac{(\tilde{A}^{(1)})^2F_{\frac{1}{2}}^{(1)}F_{\frac{1}{2}}^{(1)}F_{-\frac{1}{2}}^{(2)}}{\pi^{3/2}t^2} - \frac{\tilde{A}^{(1)}\tilde{A}^{(2)}F_{\frac{1}{2}}^{(1)}F_{\frac{1}{2}}^{(1)}F_{-\frac{1}{2}}^{(2)}}{\pi^{3/2}t^2} \\ + \frac{3\tilde{A}^{(1)}F_{\frac{1}{2}}^{(1)}F_{\frac{1}{2}}^{(1)}F_{-\frac{1}{2}}^{(2)}}{\pi^{3/2}t^2} + \frac{3\tilde{A}^{(2)}F_{\frac{1}{2}}^{(1)}F_{\frac{1}{2}}^{(1)}F_{-\frac{1}{2}}^{(2)}}{2\pi^{3/2}t^2} - \frac{9F_{\frac{3}{2}}^{(1)}F_{\frac{3}{2}}^{(1)}F_{-\frac{1}{2}}^{(2)}}{4\pi^{3/2}t^2} - \frac{(\tilde{A}^{(1)})^2F_{-\frac{1}{2}}^{(1)}F_{\frac{1}{2}}^{(1)}F_{\frac{1}{2}}^{(2)}}{\pi^{3/2}t^2}$$

$$\begin{aligned}
& + \frac{\tilde{A}^{(1)} F_{\frac{1}{2}}^{(1)} F_{\frac{1}{2}}^{(1)} F_{\frac{1}{2}}^{(2)}}{\pi^{3/2} t^2} + \frac{3\tilde{A}^{(1)} F_{-\frac{1}{2}}^{(1)} F_{\frac{3}{2}}^{(1)} F_{\frac{1}{2}}^{(2)}}{2\pi^{3/2} t^2} - \frac{3F_{\frac{3}{2}}^{(1)} F_{\frac{1}{2}}^{(1)} F_{\frac{1}{2}}^{(2)}}{2\pi^{3/2} t^2} - \frac{3\tilde{A}^{(1)} \tilde{A}^{(2)} F_{\frac{1}{2}}^{(1)} F_{-\frac{1}{2}}^{(2)} F_{\frac{1}{2}}^{(2)}}{\sqrt{2}\pi^{3/2} t^2} \\
& - \frac{5(\tilde{A}^{(2)})^2 F_{\frac{1}{2}}^{(1)} F_{-\frac{1}{2}}^{(2)} F_{\frac{1}{2}}^{(2)}}{2\sqrt{2}\pi^{3/2} t^2} + \frac{9\tilde{A}^{(2)} F_{\frac{3}{2}}^{(1)} F_{-\frac{1}{2}}^{(2)} F_{\frac{1}{2}}^{(2)}}{2\sqrt{2}\pi^{3/2} t^2} - \frac{5\tilde{A}^{(1)} \tilde{A}^{(2)} F_{-\frac{1}{2}}^{(1)} F_{\frac{1}{2}}^{(2)} F_{\frac{1}{2}}^{(2)}}{2\sqrt{2}\pi^{3/2} t^2} \\
& - \frac{(\tilde{A}^{(2)})^2 F_{-\frac{1}{2}}^{(1)} F_{\frac{1}{2}}^{(2)} F_{\frac{1}{2}}^{(2)}}{2\sqrt{2}\pi^{3/2} t^2} + \frac{\tilde{A}^{(1)} F_{\frac{1}{2}}^{(1)} F_{\frac{1}{2}}^{(2)} F_{\frac{1}{2}}^{(2)}}{\sqrt{2}\pi^{3/2} t^2} + \frac{\tilde{A}^{(2)} F_{\frac{1}{2}}^{(1)} F_{\frac{1}{2}}^{(2)} F_{\frac{1}{2}}^{(2)}}{2\sqrt{2}\pi^{3/2} t^2} + \frac{\sqrt{2}\tilde{A}^{(2)} F_{\frac{1}{2}}^{(1)} F_{\frac{1}{2}}^{(2)} F_{\frac{1}{2}}^{(2)}}{\pi^{3/2} t^2} \\
& - \frac{3F_{\frac{3}{2}}^{(1)} F_{\frac{1}{2}}^{(2)} F_{\frac{1}{2}}^{(2)}}{2\sqrt{2}\pi^{3/2} t^2} - \frac{5(\tilde{A}^{(2)})^2 F_{-\frac{1}{2}}^{(2)} F_{\frac{1}{2}}^{(2)} F_{\frac{1}{2}}^{(2)}}{8\pi^{3/2} t^2} + \frac{\tilde{A}^{(2)} F_{\frac{1}{2}}^{(2)} F_{\frac{1}{2}}^{(2)} F_{\frac{1}{2}}^{(2)}}{4\pi^{3/2} t^2} + \frac{3\tilde{A}^{(1)} F_{\frac{1}{2}}^{(1)} F_{-\frac{1}{2}}^{(2)} F_{\frac{3}{2}}^{(2)}}{2\sqrt{2}\pi^{3/2} t^2} \\
& + \frac{15\tilde{A}^{(2)} F_{\frac{1}{2}}^{(1)} F_{-\frac{1}{2}}^{(2)} F_{\frac{3}{2}}^{(2)}}{4\sqrt{2}\pi^{3/2} t^2} - \frac{9F_{\frac{3}{2}}^{(1)} F_{-\frac{1}{2}}^{(2)} F_{\frac{3}{2}}^{(2)}}{4\sqrt{2}\pi^{3/2} t^2} + \frac{15\tilde{A}^{(1)} F_{-\frac{1}{2}}^{(1)} F_{\frac{1}{2}}^{(2)} F_{\frac{3}{2}}^{(2)}}{4\sqrt{2}\pi^{3/2} t^2} + \frac{3\tilde{A}^{(2)} F_{-\frac{1}{2}}^{(1)} F_{\frac{1}{2}}^{(2)} F_{\frac{3}{2}}^{(2)}}{2\sqrt{2}\pi^{3/2} t^2} \\
& - \frac{15F_{\frac{1}{2}}^{(1)} F_{\frac{1}{2}}^{(2)} F_{\frac{3}{2}}^{(2)}}{4\sqrt{2}\pi^{3/2} t^2} + \frac{9\tilde{A}^{(2)} F_{-\frac{1}{2}}^{(2)} F_{\frac{1}{2}}^{(2)} F_{\frac{3}{2}}^{(2)}}{8\pi^{3/2} t^2} - \frac{3F_{\frac{1}{2}}^{(2)} F_{\frac{1}{2}}^{(2)} F_{\frac{3}{2}}^{(2)}}{8\pi^{3/2} t^2} - \frac{9F_{-\frac{1}{2}}^{(1)} F_{\frac{3}{2}}^{(2)} F_{\frac{3}{2}}^{(2)}}{8\sqrt{2}\pi^{3/2} t^2} - \frac{9F_{-\frac{1}{2}}^{(2)} F_{\frac{3}{2}}^{(2)} F_{\frac{3}{2}}^{(2)}}{32\pi^{3/2} t^2}, \tag{S51}
\end{aligned}$$

$$\begin{aligned}
\frac{\partial^2 \tilde{p}}{\partial \mu \partial t} &= \frac{1}{2\sqrt{2}\pi} \frac{\tilde{A}^{(1)} F_{-\frac{1}{2}}^{(1)}}{t} - \frac{1}{4\sqrt{2}\pi} \frac{F_{\frac{1}{2}}^{(1)}}{t} + \frac{1}{\sqrt{\pi}} \frac{\tilde{A}^{(2)} F_{-\frac{1}{2}}^{(2)}}{t} - \frac{1}{2\sqrt{\pi}} \frac{F_{\frac{1}{2}}^{(2)}}{t} + \frac{\tilde{A}^{(1)} F_{-\frac{1}{2}}^{(1)} F_{\frac{1}{2}}^{(1)}}{2\pi t} - \frac{F_{\frac{1}{2}}^{(1)} F_{\frac{1}{2}}^{(1)}}{4\pi t} \\
& + \frac{\sqrt{2}\tilde{A}^{(1)} F_{\frac{1}{2}}^{(1)} F_{-\frac{1}{2}}^{(2)}}{\pi t} + \frac{\tilde{A}^{(2)} F_{\frac{1}{2}}^{(1)} F_{-\frac{1}{2}}^{(2)}}{\sqrt{2}\pi t} - \frac{3F_{\frac{3}{2}}^{(1)} F_{-\frac{1}{2}}^{(2)}}{\sqrt{2}\pi t} + \frac{\tilde{A}^{(1)} F_{-\frac{1}{2}}^{(1)} F_{\frac{1}{2}}^{(2)}}{\sqrt{2}\pi t} + \frac{\tilde{A}^{(2)} F_{-\frac{1}{2}}^{(1)} F_{\frac{1}{2}}^{(2)}}{2\sqrt{2}\pi t} - \frac{F_{\frac{1}{2}}^{(1)} F_{\frac{1}{2}}^{(2)}}{\sqrt{2}\pi t} \\
& + \frac{5\tilde{A}^{(2)} F_{-\frac{1}{2}}^{(2)} F_{\frac{1}{2}}^{(2)}}{2\pi t} - \frac{F_{\frac{1}{2}}^{(2)} F_{\frac{1}{2}}^{(2)}}{\pi t} - \frac{3F_{-\frac{1}{2}}^{(1)} F_{\frac{3}{2}}^{(2)}}{4\sqrt{2}\pi t} - \frac{3F_{-\frac{1}{2}}^{(2)} F_{\frac{3}{2}}^{(2)}}{4\pi t} + \frac{\tilde{A}^{(1)} F_{\frac{1}{2}}^{(1)} F_{\frac{1}{2}}^{(1)} F_{-\frac{1}{2}}^{(2)}}{\pi^{3/2} t} - \frac{3F_{\frac{1}{2}}^{(1)} F_{\frac{1}{2}}^{(1)} F_{-\frac{1}{2}}^{(2)}}{2\pi^{3/2} t} \\
& + \frac{11\tilde{A}^{(1)} F_{-\frac{1}{2}}^{(1)} F_{\frac{1}{2}}^{(1)} F_{\frac{1}{2}}^{(2)}}{4\pi^{3/2} t} + \frac{\tilde{A}^{(2)} F_{-\frac{1}{2}}^{(1)} F_{\frac{1}{2}}^{(1)} F_{\frac{1}{2}}^{(2)}}{2\pi^{3/2} t} - \frac{9F_{\frac{1}{2}}^{(1)} F_{\frac{1}{2}}^{(1)} F_{\frac{1}{2}}^{(2)}}{8\pi^{3/2} t} - \frac{3F_{-\frac{1}{2}}^{(1)} F_{\frac{3}{2}}^{(1)} F_{\frac{1}{2}}^{(2)}}{4\pi^{3/2} t} \\
& + \frac{\tilde{A}^{(1)} F_{\frac{1}{2}}^{(1)} F_{-\frac{1}{2}}^{(2)} F_{\frac{1}{2}}^{(2)}}{\sqrt{2}\pi^{3/2} t} + \frac{2\sqrt{2}\tilde{A}^{(1)} F_{\frac{1}{2}}^{(1)} F_{-\frac{1}{2}}^{(2)} F_{\frac{1}{2}}^{(2)}}{\pi^{3/2} t} + \frac{13\tilde{A}^{(2)} F_{\frac{1}{2}}^{(1)} F_{-\frac{1}{2}}^{(2)} F_{\frac{1}{2}}^{(2)}}{2\sqrt{2}\pi^{3/2} t} + \frac{\sqrt{2}\tilde{A}^{(2)} F_{\frac{1}{2}}^{(1)} F_{-\frac{1}{2}}^{(2)} F_{\frac{1}{2}}^{(2)}}{\pi^{3/2} t} \\
& - \frac{15F_{\frac{3}{2}}^{(1)} F_{-\frac{1}{2}}^{(2)} F_{\frac{1}{2}}^{(2)}}{2\sqrt{2}\pi^{3/2} t} + \frac{\tilde{A}^{(1)} F_{-\frac{1}{2}}^{(1)} F_{\frac{1}{2}}^{(2)} F_{\frac{1}{2}}^{(2)}}{2\sqrt{2}\pi^{3/2} t} + \frac{5\tilde{A}^{(2)} F_{-\frac{1}{2}}^{(1)} F_{\frac{1}{2}}^{(2)} F_{\frac{1}{2}}^{(2)}}{4\sqrt{2}\pi^{3/2} t} - \frac{13F_{\frac{1}{2}}^{(1)} F_{\frac{1}{2}}^{(2)} F_{\frac{1}{2}}^{(2)}}{4\sqrt{2}\pi^{3/2} t} + \frac{3\tilde{A}^{(2)} F_{-\frac{1}{2}}^{(2)} F_{\frac{1}{2}}^{(2)} F_{\frac{1}{2}}^{(2)}}{\pi^{3/2} t} \\
& - \frac{7F_{\frac{1}{2}}^{(2)} F_{\frac{1}{2}}^{(2)} F_{\frac{1}{2}}^{(2)}}{8\pi^{3/2} t} - \frac{3F_{-\frac{1}{2}}^{(1)} F_{\frac{1}{2}}^{(1)} F_{\frac{3}{2}}^{(2)}}{4\pi^{3/2} t} - \frac{15F_{\frac{1}{2}}^{(1)} F_{-\frac{1}{2}}^{(2)} F_{\frac{3}{2}}^{(2)}}{4\sqrt{2}\pi^{3/2} t} - \frac{15F_{-\frac{1}{2}}^{(1)} F_{\frac{1}{2}}^{(2)} F_{\frac{3}{2}}^{(2)}}{8\sqrt{2}\pi^{3/2} t} - \frac{15F_{-\frac{1}{2}}^{(2)} F_{\frac{1}{2}}^{(2)} F_{\frac{3}{2}}^{(2)}}{8\pi^{3/2} t}, \tag{S52}
\end{aligned}$$

$$\begin{aligned}
\frac{\partial^2 \tilde{p}}{\partial h \partial t} &= \frac{\tilde{A}^{(1)} F_{-\frac{1}{2}}^{(1)}}{4\sqrt{2}\pi t} - \frac{F_{\frac{1}{2}}^{(1)}}{8\sqrt{2}\pi t} + \frac{\tilde{A}^{(1)} F_{-\frac{1}{2}}^{(1)} F_{\frac{1}{2}}^{(1)}}{4\pi t} - \frac{F_{\frac{1}{2}}^{(1)} F_{\frac{1}{2}}^{(1)}}{8\pi t} + \frac{\tilde{A}^{(2)} F_{\frac{1}{2}}^{(1)} F_{-\frac{1}{2}}^{(2)}}{2\sqrt{2}\pi t} + \frac{\tilde{A}^{(2)} F_{-\frac{1}{2}}^{(1)} F_{\frac{1}{2}}^{(2)}}{4\sqrt{2}\pi t} + \frac{\tilde{A}^{(1)} F_{\frac{1}{2}}^{(1)} F_{\frac{1}{2}}^{(1)} F_{-\frac{1}{2}}^{(2)}}{2\pi^{3/2} t} \\
& - \frac{3F_{\frac{1}{2}}^{(1)} F_{\frac{3}{2}}^{(1)} F_{-\frac{1}{2}}^{(2)}}{4\pi^{3/2} t} + \frac{7\tilde{A}^{(1)} F_{-\frac{1}{2}}^{(1)} F_{\frac{1}{2}}^{(1)} F_{\frac{1}{2}}^{(2)}}{8\pi^{3/2} t} + \frac{\tilde{A}^{(2)} F_{-\frac{1}{2}}^{(1)} F_{\frac{1}{2}}^{(1)} F_{\frac{1}{2}}^{(2)}}{4\pi^{3/2} t} - \frac{5F_{\frac{1}{2}}^{(1)} F_{\frac{1}{2}}^{(1)} F_{\frac{1}{2}}^{(2)}}{16\pi^{3/2} t} - \frac{3F_{-\frac{1}{2}}^{(1)} F_{\frac{3}{2}}^{(1)} F_{\frac{1}{2}}^{(2)}}{8\pi^{3/2} t} \\
& + \frac{5\tilde{A}^{(2)} F_{\frac{1}{2}}^{(1)} F_{-\frac{1}{2}}^{(2)} F_{\frac{1}{2}}^{(2)}}{4\sqrt{2}\pi^{3/2} t} + \frac{\tilde{A}^{(2)} F_{-\frac{1}{2}}^{(1)} F_{\frac{1}{2}}^{(2)} F_{\frac{1}{2}}^{(2)}}{8\sqrt{2}\pi^{3/2} t} - \frac{F_{\frac{1}{2}}^{(1)} F_{\frac{1}{2}}^{(2)} F_{\frac{1}{2}}^{(2)}}{2\sqrt{2}\pi^{3/2} t} - \frac{3F_{-\frac{1}{2}}^{(1)} F_{\frac{1}{2}}^{(1)} F_{\frac{3}{2}}^{(2)}}{8\pi^{3/2} t} - \frac{3F_{\frac{1}{2}}^{(1)} F_{-\frac{1}{2}}^{(2)} F_{\frac{3}{2}}^{(2)}}{8\sqrt{2}\pi^{3/2} t} \\
& - \frac{3F_{-\frac{1}{2}}^{(1)} F_{\frac{1}{2}}^{(2)} F_{\frac{3}{2}}^{(2)}}{16\sqrt{2}\pi^{3/2} t}, \tag{S53}
\end{aligned}$$

$$\begin{aligned}
\frac{\partial^2 \tilde{p}}{\partial \mu \partial h} &= -\frac{F_{-\frac{1}{2}}^{(1)}}{4\sqrt{2}\pi} - \frac{F_{\frac{1}{2}}^{(1)} F_{-\frac{1}{2}}^{(2)}}{\sqrt{2}\pi} - \frac{F_{-\frac{1}{2}}^{(1)} F_{\frac{1}{2}}^{(2)}}{\sqrt{2}\pi} - \frac{F_{\frac{1}{2}}^{(1)} F_{\frac{1}{2}}^{(1)} F_{-\frac{1}{2}}^{(2)}}{\pi^{3/2}} - \frac{3F_{-\frac{1}{2}}^{(1)} F_{\frac{1}{2}}^{(1)} F_{\frac{1}{2}}^{(2)}}{4\pi^{3/2}} - \frac{3F_{\frac{1}{2}}^{(1)} F_{-\frac{1}{2}}^{(2)} F_{\frac{1}{2}}^{(2)}}{2\sqrt{2}\pi^{3/2}} \\
& - \frac{3F_{-\frac{1}{2}}^{(1)} F_{\frac{1}{2}}^{(2)} F_{\frac{1}{2}}^{(2)}}{2\sqrt{2}\pi^{3/2}}, \tag{S54}
\end{aligned}$$

where $F_s^{(r)} \triangleq t^s \text{Li}_s(-e^{\tilde{A}^{(r)}/t})$, $r = 1, 2$

5. QUANTUM REFRIGERATION FOR THE FREE FERMION GAS

For a low temperature quantum refrigeration, we may raise up a question what is the low temperature limit for a given temperature of the hot source in the magnetic refrigeration? In order to answer this question, we consider the simplest case, i.e. the 1D two component free Fermi gas. The grand canonical potential for this system is simply given

$$\Omega = \frac{\sqrt{2m}L}{2\hbar\sqrt{2\pi}}(k_B T)^{3/2} \left[\text{Li}_{\frac{3}{2}}(-e^{(\mu+h/2)/(k_B T)}) + \text{Li}_{\frac{3}{2}}(-e^{(\mu-h/2)/(k_B T)}) \right], \quad (\text{S55})$$

where the h is the magnetic field, μ is the chemical potential, L the scale of the system, T is the temperature, \hbar is the Planck constant and the k_B the Boltzman constant. For finding the local minimum of the entropy, we only need to solve the equation

$$\Gamma_{\text{mag}} = 0. \quad (\text{S56})$$

Using eq. (8), it is not difficult to get the condition

$$\mathcal{Y}\left(\frac{\mu+h/2}{k_B T}\right) = \mathcal{Y}\left(\frac{\mu-h/2}{k_B T}\right), \quad (\text{S57})$$

here the analytic equation $\mathcal{Y}(x) = x - \frac{\text{Li}_{1/2}(-e^x)}{2\text{Li}_{-1/2}(-e^x)}$. Next we apply the low temperature limit $k_B T \ll \mu$, which implies that $\frac{\mu+h/2}{k_B T} \gg 1$. Because the analytic property of the function $\mathcal{Y}(x)$ shows $\mathcal{Y}(x) \rightarrow \frac{\pi}{6}x^{-1}$ when $x \rightarrow \infty$, then the solution of equation (S57) at low temperature is simply $\frac{\mu-h/2}{k_B T} = x_0$, where the $x_0 \approx 1.3117$ is the only zero point of function $\mathcal{Y}(x)$. Having this solution in mind, we then have the density and the entropy from canonical thermodynamic potential (S55)

$$n = \frac{\sqrt{2m}}{2\hbar} \frac{2}{\pi} \sqrt{2\mu}, \quad \frac{S}{L} = \lambda_1 \cdot \frac{\sqrt{2m}}{2\hbar\sqrt{\pi}} k_B^{3/2} T_c^{1/2}, \quad (\text{S58})$$

where $\lambda_1 = x_0 \text{Li}_{1/2}(-e^{x_0}) - \frac{3}{2} \text{Li}_{3/2}(-e^{x_0}) \approx 1.3467$. This means that we obtain the explicit form of the density and entropy at the minimum point of the temperature for an isentropic process. We also observe that at this critical point, the entropy is of order $O(T^{1/2})$ and independent of the density. In the expression eq. (S58), T_c denotes the temperature at the minimum of the entropy. We can take eq. (S58) as the state function of the D in the refrigeration cycle depicted in Fig.1. Whereas the point C , which determines the temperature of the heat source, locates deeply in the Tomonaga-Luttinger liquid (TLL) region. From the results of Luttinger liquid [20, 29], we have the following relation among the density, entropy and temperature

$$\frac{nS}{L} = \frac{m}{3\hbar^2} k_B^2 T_F, \quad (\text{S59})$$

here T_F denotes the initial temperature of the free fermions. The expressions (S58) and (S59) directly build up a useful relation between the temperatures at the minimum entropy and at any state in the TLL region through an isentropic process, namely,

$$\frac{T_c}{T_d} \approx \lambda_2^2 \cdot \left(\frac{T_F}{T_d} \right)^2. \quad (\text{S60})$$

Here the $T_d = \frac{2\pi\hbar^2 n^2}{mk_B}$ is the degenerate temperature and $\lambda_2 = 2\pi/3\lambda_1 \approx 1.5552$ is a constant. The relation (S60) gives the lowest limit of the temperature for a magnetic refrigeration with a fixed temperature of the heat source. We see clearly that in the quantum gases the thermal wave length is usually much smaller than its de Broglie wave length. We always have a relation $T_F \ll T_d$ [61]. Therefore, according to (S60), we have $T_c \ll T_F \ll T_d$. Here T_F is the Fermi temperature of the heat source, i.e. $T_F \rightarrow T_{\text{sour}}$. Whereas the T_c is the temperature of the target system, i.e. $T_c \rightarrow T_{\text{tar}}$, see Fig. 4 in the main text. We ought to point out that the equation (S60) holds only in the case that the temperature T_F is lower than the temperature of quantum degenerate temperature T_d .